STRUCTURE AND PETROLOGY OF A PART OF THE EAST FLANK OF THE SANTA CATALINA MOUNTAINS, PIMA COUNTY, ARIZONA

by

Harold Dean Pilkington

A Dissertation Submitted to the Faculty of the

DEPARTMENT OF GEOLOGY

In Partial Fulfillment of the Requirements
For the Degree of

Doctor of Philosophy

In the Graduate College

THE UNIVERSITY OF ARIZONA

1962

THE UNIVERSITY OF ARIZONA

GRADUATE COLLEGE

I hereby recommend that this dissertation prepared under my direction by Harold Dean Pilkington

entitled STRUCTURE AND PETROLOGY OF A PART OF THE EAST FLANK OF THE SANTA CATALINA MOUNTAINS, PIMA COUNTY, ARIZONA

be accepted as fulfilling the dissertation requirement of the degree of Doctor of Philosophy

R. H. Brown — 6-25-62

Dissertation Director — Date

After inspection of the dissertation, the following members of the Final Examination Committee concur in its approval and recommend its acceptance:*

Evans B. Mayo	6-25-62
John F. Lance	6-25-62
W. L. Lacy	6-26-62
John W. Cutbirth	6/26/62

*This approval and acceptance is contingent on the candidate's adequate performance and defense of this dissertation at the final oral examination. The inclusion of this sheet bound into the library copy of the dissertation is evidence of satisfactory performance at the final examination.

STATEMENT BY AUTHOR

This thesis has been submitted in partial fulfillment of requirements for an advanced degree at the University of Arizona and is deposited in the University Library to be made available to borrowers under rules of the Library.

Brief quotations from this thesis are allowable without special permission, provided that accurate acknowledgement of source is made. Requests of permission for extended quotation from or reproduction of this manuscript in whole or in part may be granted by the head of the major department or the Dean of the Graduate College when in their judgment the proposed use of the material is in the interests of scholarship. In all other instances, however, permission must be obtained from the author.

SIGNED: W. D. Pilkington

STRUCTURE AND PETROLOGY OF A PART OF THE EAST FLANK OF THE SANTA CATALINA MOUNTAINS, PIMA COUNTY, ARIZONA

by

H. D. Pilkington

ABSTRACT

The Santa Catalina Mountains consist of a gneissic core flanked by metasedimentary rocks. The granitic gneiss and banded augen gneiss which make up the core are transitional between the kyanite-muscovite-almandine subfacies and the staurolite-almandine subfacies of regional metamorphism. Younger Precambrian and Paleozoic metasedimentary rocks occur along the eastern flank of the mountains. The Younger Precambrian Apache Group includes the Pioneer Formation, Dripping Spring Quartzite, and Mescal Limestone all of which have been converted into rocks of the staurolite-almandine subfacies. The Paleozoic sections consists of the Bolsa Quartzite, Abrigo Limestone, and a small area of undifferentiated Paleozoic limestones which have been affected by a similar grade of metamorphism. Dikes and sills of metamorphosed quartz latite prophyry are abundant in the metasedimentary rocks. Post-kinematic replacement pegmatites and aplites are found in the rocks of the Apache Group and the gneissic complex.

Two dominant structural directions occur in the Catalina Mountains. The strike of the foliation and major fold axes have a west-northwest trend. The "b" lineation associated with crinkled foliation and elongated pebbles in the Apache Group and the elongated augen and streaked micas of the gneisses along the crest and eastern slopes trends west-northwest. A northeast direction is characterized by lineation of "a" related to superimposed cataclasis.

The metamorphism and development of the structural features has been related to the formation of a mantled gneiss dome. It is suggested that the dome formed during the Laramide Orogeny.

TABLE OF CONTENTS

Page

LIST OF ILLUSTRATIONS

Figures

Figure Page

Figure Page

Figure Page

Tables

Plates

INTRODUCTION

Purpose and Methods of Investigation

The purpose of this investigation is to contribute information on the structure and petrology of the Santa Catalina Mountains, Arizona. The lithologic units were traced from the summit region of the mountains northeastward along the flank of the mountains. Detailed structural studies were made to determine the significance of the two directions of lineation reported by Peirce (1958) and DuBois (1959), the nature of the foliation, and the joint patterns. Petrographic descriptions were made of all the lithologic units exposed within the area of study. Based upon the above investigations, an explanation is offered of the petrogenesis of the area.

A structural and geologic map was prepared on an enlargement of the 1957 U. S. Geological Survey topographic map of the Bellota Ranch Quadrangle, Pima County, Arizona. An area of 30 square miles was mapped on a scale of four inches to the mile. Aerial photographs having a scale of one inch to the mile, and when they became available photos having a scale of four inches to the mile, were used to facilitate accurate plotting of information. Laboratory studies included mineralogic determinations based upon specific gravity, index of refraction, and X-ray diffraction techniques. Petrographic investigations included thin section examination, modal analysis, and universal stage techniques.

Location and Accessibility

The Santa Catalina Mountains form the northwestern extension of a larger range which includes the Tanque Verde and Rincon Mountains. The range is located in Pima and Pinal Counties, Arizona, and forms the eastern and northeastern borders of the valley in which Tucson is located (Fig. 1). The mountain range is approximately forty miles long and from five to twenty miles wide. The map area extends from the crestal regions of the Catalina Mountains, in the vicinity of the Palisades Ranger Station, eastward across the northeast flank along Buehman Canyon and its tributaries. Access to the western side of the area is gained by the Mount Lemmon highway while the eastern part may be reached by means of "jeep" trails from the San Pedro Valley near Reddington, Arizona.

Topography and Physiography

The Santa Catalina Mountains rise abruptly from valleys on the eastern and western sides. The Catalina Mountains, Tanque Verde Mountains, and Rincon Mountains form one of the ranges within the Basin and Range Province of southern Arizona. The maximum elevation within the area of investigation is the summit of Kellogg Mountain at about 8,400 feet and the minimum elevation is in Buehman Canyon at 3,360 feet. The maximum relief, therefore, is approximately 5,000 feet (Plate IV).

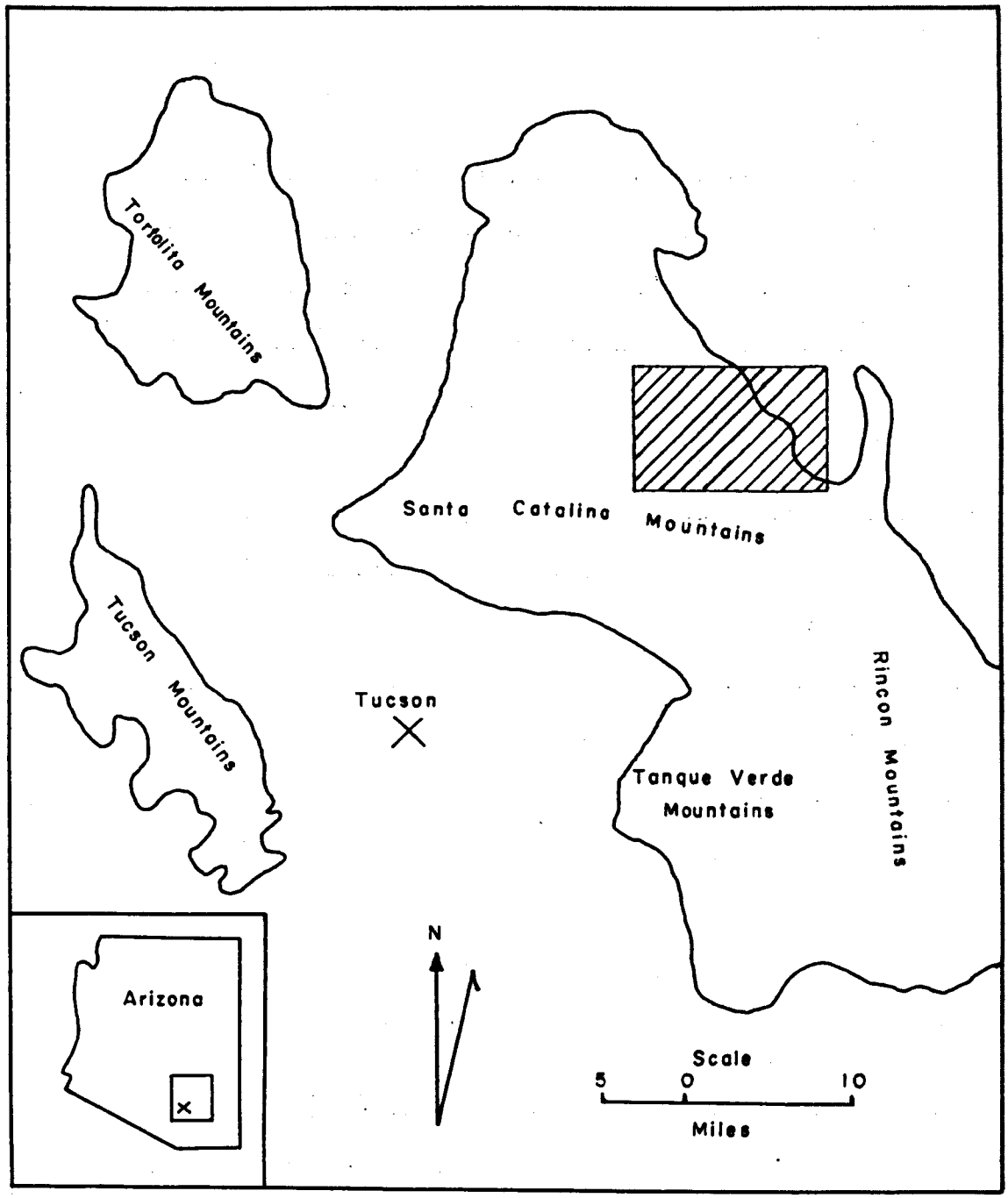

Figure 1. Index map showing location of the area of present study.

The Catalina Mountains are well dissected by intermittent streams. The western third of the area drains into Sabino and Bear Canyons and thence to the Santa Cruz River. The eastern side is drained by Buehman Canyon and its tributaries which flow into the San Pedro Valley.

Previous Work

The number of published accounts of previous geologic investigations in the Santa Catalina Mountains is very limited. Among the earliest was that by Darton in 1925. The geomorphology was discussed by Davis (1931). Bromfield (1952) summarized the geology of the Catalina Mountains. The geologic setting of the Santa Catalina Mountains and the petrography of a part of the gneissic complex were described by DuBois (1959). A mineralogic investigation of some garnets from the Santa Catalina Mountains was made by the author (1961).

Several unpublished investigations provide data on the geologic features. A U.S. Geological Survey open file report by Moore and Tolman (1949) on the geology of the Tucson Quadrangle covers the area of the present study. Theses by University of Arizona graduate students also provide data on limited areas. Wallace (1954) discussed the stratigraphy and structure along the Mogul Fault. Banerjee (1957) worked on the structure and petrology of the Oracle Granite. The structure and petrography of the north-central portion of the Santa Catalina Mountains was studied by Peirce (1958). Raabe (1959) described the

geology of the Bullock Canyon area. The petrology of the Molino Basin area of the Santa Catalina Mountains was described by Laughlin (1959). The use of sodium-potassium ratios in muscovites as a geothermometer was discussed by Hedge (1960) for a limited number of Catalina rocks. The Younger Precambrian geology of southern Arizona has been discussed in some detail by Shride (1961). Jinks (1961) did a detailed study of a portion of the Mogul Fault. The structure and petrography of the Pinal Schist south of the Mogul Fault was described by Erickson (1962).

Acknowledgements

The author wishes to express his sincere appreciation to Dr. R. L. DuBois for his aid and encouragement throughout all stages of this investigation. Field trips and numerous discussions with Dr. Evans B. Mayo were invaluable in developing ideas on tectonics. Discussions with other graduate students have been very beneficial, especially those with E. J. McCullough, Jr. The critical reading of the manuscript by Professors W. C. Lacy, J. W. Anthony, S. R. Titley, and E. B. Mayo is gratefully acknowledged. Finally the author wishes to express his sincere thanks for the courtesies extended to him by the rangers of the Coronado National Forest.

GENERAL GEOLOGY

The geologic setting of the Santa Catalina Mountains is given so that the results of the present investigation may be referred to the overall picture. The Mountains are made up of a complex of igneous, metamorphic, and sedimentary rocks. The core consists of gneissic granite. On the southwest slopes the core is flanked by augen gneiss and banded augen gneiss. The northeastern side is bounded by banded augen gneiss and metasedimentary rocks (Plate I). The gross structural feature of the mountains is a large gneiss dome which is elongated in a west-northwest direction. Minor folds and domes are found on the large domal structure. Numerous faults have been observed and some mapped in detail. Two directions of linear features have been observed and were studied in some detail in the present investigation.

Description of Rocks

Older Precambrian

Pinal Schist

The oldest rocks exposed in the Santa Catalina Mountains are Pinal Schist. The metasediments of the Pinal Schist crop out extensively in the northern part of the Catalinas (Wallace, 1954) and minor exposures in the central portion were described by Peirce (1958). The rocks south of the Mogul Fault, discussed by Erickson (1962), are typified by phyllites and muscovite

schists which exhibit rather strong crenulation of the foliation. The banded augen gneisses exposed on the northeastern slopes of the area of the present study are believed, by the author, to have been formed in part from the Pinal Schist.

Oracle Granite

The granite which forms the northern part of the range has been named the Oracle Granite. The granite intrudes the Pinal Schist or is in fault contact with either Younger Precambrian or Paleozoic rocks. The Oracle Granite is a coarse-grained porphyritic quartz monzonite with local variations. Banerjee (1957) considered that the rock was originally of granodioritic composition and was later changed by potassium metasomatism. Banerjee regarded the Oracle Granite to be of Precambrian age. Geochemical dating of biotite from the granite gives an Older Precambrian age of 1,450 m.y. (Damon, 1959).

Younger Precambrian

Apache Group

The Younger Precambrian Apache Group crops out extensively in the northern and central regions of the Santa Catalina Mountains. The distribution of the metasediments has been recorded in some detail by Wallace (1954) and Peirce (1958). The problem of the distribution and nature of the Apache Group along the summit and eastern slopes of the mountains is a part of the present study and will be discussed later. Raabe (1959)

described the character of the Younger Precambrian rocks in the Bullock Canyon area. The rocks of the Apache Group will be broken down according to the proposal of Shride (1961).

Pioneer Formation

The lowermost unit of the Apache Group is the Pioneer Formation. The basal conglomerate, which ranges from 0 to 50 feet in thickness, is termed the Scanlan Conglomerate Member. The Scanlan varies from a coarse sandstone to a quartzose conglomerate. In the northern part of the Catalina Mountains the low-grade metamorphism has not destroyed the original sedimentary texture. Along the crest of the mountains, however, the rocks have been converted into coarse-grained quartz-muscovite schists or quartzites (Peirce, 1958). In the Bullock Canyon area Raabe (1959) described the Scanlan Member as a conglomerate with the pebbles and cobbles greatly elongated by intense shearing and recrystallization.

The basal conglomerate grades into the overlying silty mudstones and interbedded fine-grained sandstones. The rocks of the upper member of the Pioneer Formation in the northern part of the mountains have been slightly metamorphosed and are typified by a phyllitic sheen. Peirce (1958) reports that the Pioneer Formation along the summit of the range has been affected by medium-grade metamorphism which developed quartz-muscovite schists.

Dripping Spring Quartzite

The basal conglomerate of the Dripping Spring Quartzite conformably overlies the Pioneer Formation. The basal conglomerate ranges from 0 to 75 feet in thickness and is known as the Barnes Conglomerate Member. The low-grade metamorphism in the northern part of the Santa Catalina Mountains resulted in a preferred orientation of the sericite in the matrix but did not destroy the original sedimentary characteristics. The medium-grade metamorphism to the south developed elongated pebbles and cobbles set in a matrix of well-oriented muscovite and biotite, and highly sutured quartz (Peirce, 1958).

The Barnes grades upward into interbedded sandstones and siltstones. The weakly metamorphosed areas of upper Dripping Spring Quartzite in the northern end of the Catalinas are characterized by oriented sericite and chlorite in the matrix and rounded to sub-rounded grains of quartz and feldspar (Peirce, 1958). The medium-grade metamorphic equivalents in the Summerhaven and Bullock Canyon areas consist of strongly sutured quartzites and quartz-mica-feldspar schists.

Mescal Limestone

Limited exposures of carbonate rocks in the Summerhaven and Bear Wallow areas along the crest of the Catalina Mountains have been interpreted as Mescal Limestone (Peirce, 1958). The exposures range considerably in thickness and are discontinuous along their strike.

Troy Quartzite

The Troy Quartzite of the type area has now been reassigned to the Younger Precambrian (Shride, 1961). According to current usage, the only rocks in the Santa Catalina Mountains which might correlate with the Troy Quartzite consist of a few feet of purple quartzite exposed in the northern part of the mountains (Shride, 1961). Within the mapped area the grade of metamorphism makes uncertain the recognition of rocks which might correlate with the Troy Quartzite.

Paleozoic

Sedimentary rocks of Paleozoic age crop out extensively along the northeast slopes of the Santa Catalina Mountains. The distribution has been studied in detail by Wallace (1954) and Peirce (1958). Only the basal units will be described here since rocks higher in the section were not found in the area mapped.

Bolsa Quartzite

The basal unit of the Paleozoic strata in the Santa Catalina Mountains is the Middle Cambrian Bolsa Quartzite according to Shride (1961). Stoyanow (1936) designated the lowermost unit of the Paleozoic as the Troy Quartzite and considered it to be of Middle Cambrian age. As mentioned above the Troy of the type area has been reassigned to the Younger Precambrian; therefore, the base of the Paleozoic section has been correlated with the Middle Cambrian Bolsa Quartzite.

The Bolsa Quartzite in the northern part of the mountains is characterized by medium- to coarse-grained sandstones. The grains are slightly interlocking as a result of secondary overgrowths. As the grade of metamorphism increases the rocks are typified by destruction of the overgrowths by recrystallization and the development of interlocking, sutured grain boundaries.

Abrigo Limestone

The Bolsa Quartzite is conformably overlain by 300 or more feet of mudstones, calcareous shales, and sandstones which Stoyanow (1936) named the Santa Catalina Formation. However, in the present work the rocks are designated as the Abrigo Limestone as suggested by Shride (1961). This correlation is based upon lithologic similarity with the lower unit of the Abrigo Limestone in northwestern Cochise County (Shride, 1961). The upper unit of the Abrigo found in Cochise County correlates with the "restricted" Abrigo of Stoyanow (1936). The Abrigo Limestone is Middle and Upper Cambrian in age.

The Abrigo Limestone crops out along most of the northeastern slope of the Catalina Mountains. The rocks exhibit the same changes in metamorphic grade as are illustrated by the rocks lower in the section. Peirce (1958) believed that the tremolite-biotite-staurolite schists near Mount Lemmon were the medium-grade equivalents of the lower part of the Abrigo Limestone as designated by Shride (1961).

Post Paleozoic

Catalina Gneiss

The term Catalina Gneiss has been applied to the gneissic complex which crops out in the summit regions and the southwestern flank of the Santa Catalina Mountains. The gneissic rocks have been divided into three general types by DuBois (1959): banded augen gneiss, augen gneiss, and granitic gneiss to gneissic granite. Banded augen gneisses form the outermost portion of the complex on both the southwestern and northeastern slopes of the Catalina Mountains (Plate I). The augen gneisses occupy an intermediate position and the granitic gneiss or gneissic granite forms the core of the complex. The mineralogic composition of each of the three types of gneiss is similar and consists of plagioclase, potash feldspar, quartz, muscovite, and biotite.

Leatherwood Quartz Diorite

The Leatherwood Quartz Diorite occurs as a stock-like mass on the northeastern slopes of the Santa Catalina Mountains (Peirce, 1958). The quartz diorite is reported to intrude rocks as young as Cretaceous (Bromfield, 1952). The rocks have been synkinematically metamorphosed. The mineral composition of the metamorphosed rock includes oligoclase, quartz, biotite, and epidote.

Quartz Latite Porphyry

Slightly metamorphosed quartz latite prophyry occurs as dikes and sills in the northern parts of the Catalina Mountains according to Peirce (1958). In the central and eastern portions of the range the quartz latite has been subjected to medium-grade metamorphism and consists of oligoclase, microcline, biotite, quartz, muscovite, and epidote.

Pegmatite and Aplite

Aplitic to pegmatitic quartz monzonite masses occur as dikes, sills, and irregular masses within the Younger Precambrian metasediments, the Leatherwood Quartz Diorite, and the Catalina Gneiss. Many of the bodies have relict structures parallel to the structure of the country rock which suggests a replacement origin. The aplites and pegmatities are late synkinematic and post kinematic.

Regional Structure

The topographic expression of the Santa Catalina Mountains reflects the major structural features. As shown on Plate I the main part of the Catalina Mountains trends west-northwest as do the major structural features such as faults, fold axes, foliation, and joints. In the southern part of the Catalinas the dominant structural trends are north and the topographic trend is also north. A third structural direction is northeast and is manifested by a strong lineation and a dominant joint set.

The structural features shown on Plate I represent a compilation of previous geologic mapping as well as the author's interpretation made in this study. The areas not covered in previous literature were studied on aerial photographs and the interpretations were checked by a limited number of field visits.

Faults

Several prominent faults have been observed in the Santa Catalina Mountains. The Mogul Fault mapped by Wallace (1954) and Jinks (1961) dips steeply and trends nearly west in the northern part of the mountains. A few miles to the south Peirce (1958) mapped another large west-northwest trending fault which he named the Geesman Fault. Approximately two miles further to the south Peirce found another fault whose trend is parallel to the Geesman Fault. All these faults are characterized by steep dips and have the south block downthrown.

Along the south flank of the mountains, Fair and Jinks (1961) studied the nature of the so-called "boundary fault". DuBois and Mayo (personal communication) report that Dr. R. W. Van Bemmelen has pointed out that the topographic depression along the south side of the mountains might represent a graben. The three found numerous antithetic faults in the tilted Tertiary sediments and also in the banded augen gneisses which support the suggestion. Wallace (1954) mapped the Pirate Fault along the western side of the Catalina Mountains. As the Pirate Fault is traced southward its trend changes from north to northeast.

Within the area bounded by the Mogul and Geesman Faults many northeast trending faults have been observed (Wallace, 1954). The topographic expression along the south flank of the mountains suggests, to the author, the presence of several minor northeasterly faults which would account for the minor offsets observed. Several north-northwest striking breccia zones have been observed in various parts of the western end of the Catalina Mountains.

Folds

If one considers the overall nature of the Santa Catalina Mountains it becomes apparent that the basic structure is that of an elongate dome whose axis trends west-northwest (Plate I). Minor folds are not uncommon on the larger dome. For example, Peirce (1958) mapped a large syncline south of the Geesman Fault. Several minor folds were observed in the present study and will be discussed later. Minor drag folds and crumpled or crenulated foliation are common in the rocks of the Apache Group exposed along the crest of the range. The fold axes are all parallel to the axis of the main dome. Mayo (personal communication) has mapped a series of minor west trending folds near the end of North Campbell Avenue. The folds shown on the south side of the Catalina Mountains (Plate I) represent the present author's interpretation of aerial photographs and observations made on several reconnaissance trips.

Foliation and Lineation

The foliation in the rocks of the Catalina Mountains trends west-northwest for the most part, and in general dips away on either side of the range. The foliation within the gneissic complex near the crest of the range parallels the foliation of the metasedimentary rocks. Many minor folds and domes produce irregularities in the overall pattern of the foliation. Peirce (1958) reports that the foliation within the Leatherwood Quartz Diorite is parallel to that in the gneissic rocks exposed along the summit of the mountains.

There are two general directions of linear features in the rocks of the Santa Catalina Mountains. The most obvious is the strongly developed northeasterly trending lineation in the gneissic rocks on the southwest flank of the mountains. This lineation results from the elongation of feldspar porphyroblasts, elongated quartz grains, and streaked masses of mica. The lineation was formed by rather intense cataclastic deformation. The same direction is also present in the Oracle Granite according to Banerjee (1957). The second direction of lineation is represented by west-northwest to west trending structures in the Oracle Granite, the metasediments of the Apache Group along the crest of the range, and also in the gneissic rocks near the crest of the range. Details of the west-northwest lineation found in the present study will be discussed later.

PETROGRAPHY

In the following discussion the rocks will be described in the chronological order established by Peirce (1958) and DuBois (1959). Thus the metamorphosed equivalents of the Apache Group are discussed under the heading of Younger Precambrian rocks, although their present characteristics were imparted to them by a much later metamorphism. Likewise the rocks of the gneissic complex, which probably represent geologically older rocks, will be discussed under the heading of Post-Paleozoic rocks.

The petrographic descriptions include both the megascopic and microscopic features of the rocks. Over 400 thin sections were prepared from specimens collected from the various lithologic units. Mineral identifications are based upon routine thin section techniques unless otherwise noted. The modal analyses were run by the point count method using a modified mechanical stage with a minimum grid interval of one-half millimeter. The weight percentages of the various oxides were calculated from the modal analyses by means of the tables given in Johannsen (1939).

Younger Precambrian

Apache Group

The Apache Group of Younger Precambrian age crops out nearly continuously along the northeastern flank of the Santa Catalina Mountains in the map area (Plate II). The section is

not everywhere complete, and the thickness of individual members changes considerably along the strike. The terminology proposed by Shride (1961) has been adopted.

Pioneer Formation

Within the mapped area, the lowermost unit of the Apache Group rests unconformably upon the granitic gneiss along the crest of the range, and is unconformable upon the banded augen gneiss elsewhere. The Scanlan Member, the basal conglomerate, appears in discontinuous outcrops as a result of either non-deposition or erosion. The basal unit varies from a coarse sandstone to a quartzitic conglomerate.

Megascopically the Scanlan Conglomerate of the Pioneer Formation is quite variable. The color varies from a white to a pinkish gray, dependent upon the nature of the contained iron. The coloration may be a result of either limonitic stain or hematitic stain. The grain size ranges from a coarse sandstone, with small pebbles scattered irregularly along the bedding planes, to a cobble conglomerate with a sandy matrix. The large clastic fragments range from pebbles one-half an inch in diameter to cobbles up to six inches in diameter. The particles of the coarse-grained sandstones and also the smaller pebbles consist of clear, glassy quartz. The colorless quartz grains are often surrounded by an iron oxide stain, and may have fractures filled with iron oxide. Some of the smaller pebbles and most of the larger cobbles are detrital rock fragments of metaquartzite.

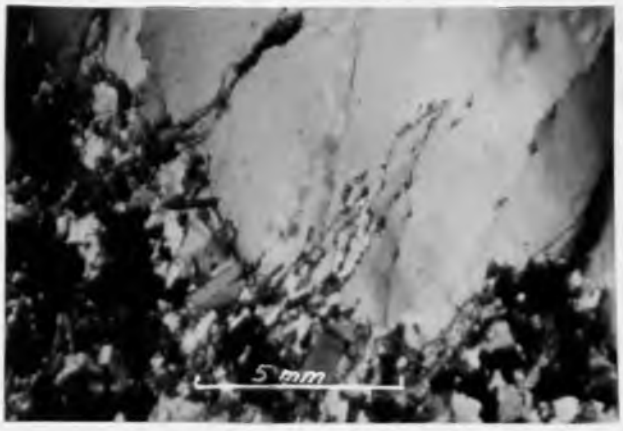

Figure 2. Photomicrograph of a sheared quartzite pebble in the Scanlan Conglomerate from Buehman Canyon. Shear planes within the pebble are parallel to the foliation within the matrix. Nicols crossed.

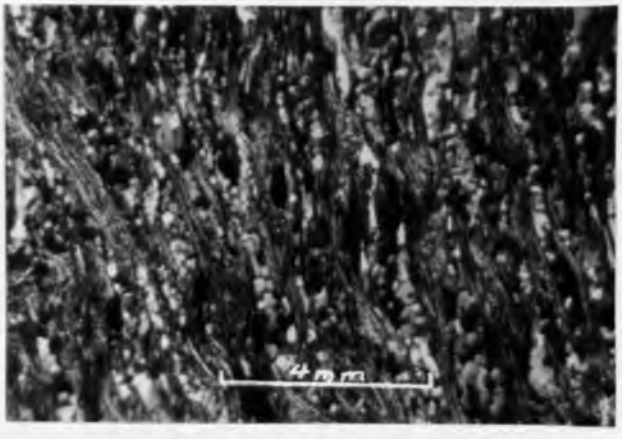

Figure 3. Subparallel orientation of muscovite which outlines the wavy foliation in a quartz-muscovite schist from the upper part of the Pioneer Formation near the summit of the Catalina Mountains. Crossed Nicols.

The quartzite fragments are well-rounded and occur in a matrix of rounded to sub-angular quartz grains and oriented mica flakes. The color of the quartzite fragments varies from nearly colorless to light gray or buff. The quartzite fragments are quite conspicuous in the matrix of colorless glassy quartz grains. The pebbles and cobbles are usually somewhat elongated and in extreme cases they have been drawn out into cigar-shaped masses which have a major axis of at least six times that of the minor axis.

Microscopically the Scanlan Conglomerate is composed of quartz, feldspar, muscovite, biotite, and epidote. Minor accessory minerals include magnetite, zircon, sphene, apatite, and garnet. Quartz comprises 75 to 80 per cent of the rock. The quartz grains in the coarse-grained quartzites and those in the matrix of the conglomerates are extensively recrystallized as evidenced by their strongly sutured contacts. The majority of the pebbles and cobbles are composed of sheared and recrystallized metaquartzite. The shearing within the quartzite fragments is parallel to the foliation and to the elongation of the grains in the matrix (Fig.2).

Feldspars make up from 0 to 15 per cent of the Scanlan Conglomerate Member. Microcline exhibits the typical grid twinning while the plagioclase crystals are usually untwinned. The plagioclase has a composition of oligoclase (An_{21}) as determined by the Michel Levy method. The mica content varies from 2 to 15 per cent. The micas are subhedral and exhibit a

distinct parallel orientation. Muscovite is more abundant than biotite. Epidote occurs in two distinct forms. The most abundant is that of the subhedral crystalloblastic epidote which constitutes up to five per cent of the rock. Scattered throughout the unit are well-rounded cloudy grains of epidote which probably represent relict detrital fragments.

Zircon and sphene occur as sub-rounded to rounded relict detrital grains which range from 0.1 to 1.0 mm in diameter. Subhedral apatite crystals are sparsely distributed in the rock.

The mineralogic composition and textural relationships suggest that the original sedimentary rock was a mineralogically mature conglomerate (an oligomictic conglomerate according to Pettijohn, 1957). The original composition consisted of quartz, as individual grains and also as quartzite fragments, and minor amounts of clay minerals or sericite. Scattered heavy minerals including magnetite, zircon, sphene, and epidote were present. Metamorphic minerals include feldspar, micas, epidote, garnet, and apatite.

The Scanlan Conglomerate Member grades into the schistose quartzites and mica schists of the upper 200 feet of the Pioneer Formation. The upper member lies unconformably upon the granitic gneiss or banded augen gneiss whenever the Scanlan Conglomerate is missing. In the Buehman Canyon area the upper member of the Pioneer Formation has been somewhat inflated by the intrusion of several sills and dikes of diabase.

The upper member of the Pioneer Formation shows considerable variation in appearance. Along the summit of the Catalina Mountains the rocks consist of coarse-grained muscovite schists. The schists are silvery red on fresh surfaces and weather to a reddish brown. The foliation is considerably contorted and crenulated by micro-folds up to one-half an inch across. The exposures of Pioneer along Buehman Canyon consist of very fine-grained light-gray to pink argillaceous quartzites, and medium-gray mica schists. The fine grain size and abundance of sericite and fine-grained muscovite give the rock a very characteristic sheen.

Thin section analysis shows the upper member of the Pioneer Formation to consist of quartz, feldspar, muscovite, biotite, and epidote. Minor constituents are apatite, sphene, zircon, magnetite, and tourmaline. Quartz is the most abundant mineral and makes up 45 to 80 per cent of the rock. The quartz grains range from less than 0.1 mm up to 0.2 mm in size. Local exceptions are found in the recrystallized quartz grains in the axial portions of the micro-folds where the grains reach one to two millimeters in diameter. The grains exhibit moderate to strong undulatory extinction and have interlocking sutured contacts. Feldspars are usually present, but normally make up less than five per cent of the rock. Certain layers are notably more feldspathic and may contain up to 30 per cent combined feldspar. Microcline is the most abundant feldspar, but small quantites of oligoclase (An_{21}) are present.

Muscovite is the most abundant mica and constitutes 25 to 45 per cent of the schistose rocks. In the schistose quartzites, muscovite is present in smaller amounts averaging 5 to 10 per cent of the rock. The muscovite occurs as subhedral grains with subparallel to parallel orientation which outlines the minor irregularities and crenulations in the foliation (Fig. 3). Subhedral biotite flakes comprise one to five per cent of the rock. Biotite commonly develops along the cleavages in muscovite crystals. Epidote is an omnipresent mineral, but always in amounts less than five per cent.

Among the minor accessory minerals zircon appears as rounded to sub-rounded relict detrital grains. A few subhedral to euhedral zircon crystals occur as inclusions within the feldspars. Apatite in one of the most common minor minerals, and occurs as idiomorphic crystals concentrated along certain of the foliation planes. Tourmaline, pleochroic from blue-green to nearly colorless, is present as euhedral prisms up to 0.1 mm long. Magnetite as euhedral to anhedral grains makes up as much as two per cent of the rocks. Traces of rounded, detrital sphene appear in a few sections.

The results of five modal analyses are shown in Table I. Each analysis represents 500 point counts made on 0.5 mm grid interval. The weight percentages of the various oxides calculated from the modal analyses are given in Table II. When the above oxide compositions are compared with those given by Pettijohn (1957) it is seen that the composition of the Pioneer

Table I. Modal analyses of the Pioneer Formation.

Mineral	Sc 100	Sc 120	Sc 141	Sc 391	Sc 464
Quartz	45.4	60.0	69.8	75.5	85.1
Plagioclase	--	--	--	--	--
Microcline	5.0	4.9	5.1	4.6	--
Muscovite	40.9	29.8	19.8	12.8	12.8
Biotite	4.9	1.0	1.7	4.4	--
Epidote	0.8	0.9	0.8	0.7	1.0
Magnetite	1.9	1.1	1.0	1.8	1.0
Others	0.7	1.0	1.0	1.1	--
	99.6	98.7	99.2	100.9	99.9

Table II. Chemical compositions calculated from the modal analyses given in Table I.

Oxide	Sc 100	Sc 120	Sc 141	Sc 391	Sc 464
SiO2	70.0	79.8	82.3	84.7	91.2
Al_2O_3	18.0	13.9	9.7	8.5	4.8
FeO	1.3	0.1	1.4	1.2	0.7
(Mg,Fe)O	1.0	0.2	0.4	0.3	--
CaO	0.5	0.2	0.7	1.2	1.0
Na_2O	--	0.2	0.2	0.3	--
K_2O	6.1	5.3	3.3	3.1	1.2
H_2O	2.0	0.5	1.3	0.9	0.7
	98.9	100.2	99.3	100.2	99.6

rocks falls between typical sandstones and typical shales. The rocks of the Pioneer Formation are richer in silica and potassium than normal shales and lower in aluminum. The composition can be explained by assuming that the original sediment consisted of intercalated siltstones and shales. The high potash content of the first two examples, Sc 100 and Sc 120, does not appear to be compatible with either a normal siltstone or shale. Furthermore, the SiO_2 content is high, especially in the final example. If the original sediments had been deposited in a restricted basin the high potash content might be accounted for, especially if there were active volcanism or hot spring activity. Shride (1961) reports that the upper Pioneer Formation often contains recognizable tuffaceous layers. However, the degree of metamorphism in the area of the present study is such that relict volcanic textures would have been destroyed.

It might be argued that the high potash content is related to metasomatic activity, but the author disregards such a hypothesis for the following reasons. First the typical result of potassium metasomatism would be the development of potash feldspars. The existence of feldspar porphyroblasts in the Pioneer Formation adjacent to the contacts with the banded augen gneiss indicates that such a mechanism was active, but on a very limited scale. Secondly the potash feldspars, with the exception of the prophryoblasts mentioned above, appear as anhedral grains which are considerably clouded by alteration products and appear to be relict detrital grains.

Dripping Spring Quartzite

The Barnes Conglomerate Member of the Dripping Spring Quartzite is conformable with the underlying Pioneer Formation. The conglomerate ranges from 0 to 75 feet in thickness. The Barnes crops out almost continuously along the northeastern slope of the mountains (Plate II). Along the summit of the mountains the Barnes is missing as a result of either erosion or non-deposition.

Megascopically the Barnes Conglomerate is very distinctive. It is characterized by pebbles and cobbles dispersed in a matrix of finer quartz and muscovite. The pebbles and cobbles are predominantly composed of white metaquartzite, but scattered gray chert fragments and yellow-brown jasper fragments occur. The quartzite fragments range up to eight inches in diameter, but average two to four inches. The chert and jasper clasts are much smaller and average one-half to one inch in diameter. The pebbles and cobbles are commonly elongated in the rocks exposed in the eastern part of the area mapped. The major axis of the elongated fragments ranges from two to five times that of the minor axis. The color of the rock is also diagnostic, with the white quartzite fragments, gray chert clasts, and yellow-brown jasper grains dispersed in a tan or pinkish-tan matrix.

Microscopic study reveals that the Barnes Member is composed of quartz, muscovite, biotite, feldspar, epidote, and garnet. Apatite, sphene, zircon, and magnetite are the

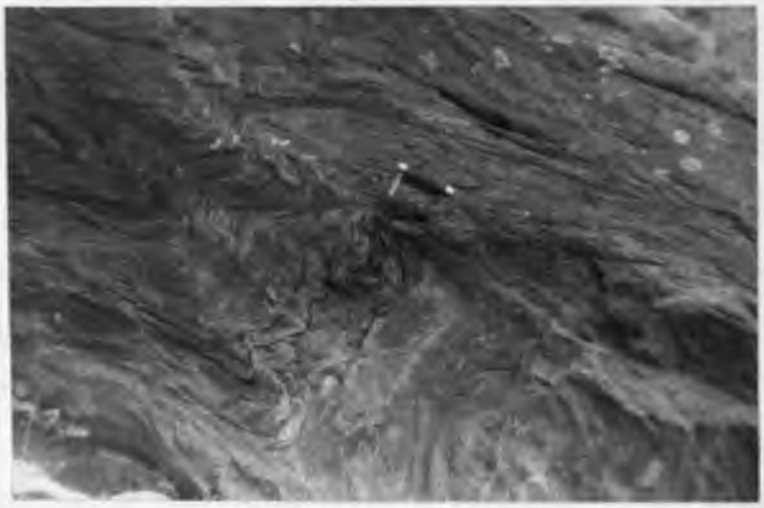

Figure 4. Minor folds in the Dripping Spring Quartzite east of Nagge Peak. The photograph was taken looking north at a nearly vertical exposure.

Figure 5. Dripping Spring Quartzite veined by aplitic and pegmatitic materials on the northeast slope of Kellogg Mountain. The photograph was taken looking west from Nagge Peak.

accessory minerals. Quartz comprises 80 to 95 per cent of the rock, and occurs in two distinct forms. The pebbles and cobbles consist of metaquartzite fragments in which the grain boundaries are strongly sutured. The quartz of the matrix is commonly of individual crystal fragments and an occasional small grain of metaquartzite. Considerable recrystallization has occurred and the majority of grains have sutured contacts.

Muscovite is a common constituent of the matrix and accounts for up to 20 per cent of the rock. The muscovite occurs as small, well-oriented plates from 0.1 to 1.0 mm in length. Biotite is not always present, but may comprise up to five per cent of the rock. Porphyroblasts of epidote exist in small quantities in all thin sections studied, and reach five per cent in a few of the rocks. Small, slightly birefringent garnets occur in very minor amounts. The small grain size, less than 0.05 mm, and limited occurrence precluded the determination of the composition of the garnet.

Magnetite and apatite are the most common accessory minerals found in the matrix. Rounded to sub-rounded, relict, detrital grains of sphene and zircon are sparsely distributed throughout the matrix.

The minerals present and the textural relationships suggest that the Barnes was originally an oligomictic conglomerate (Pettijohn, 1957). The initial rock was composed of siliceous pebbles and cobbles in a matrix of quartz and clay

minerals. Metamorphism resulted in the development of feldspars, micas, epidote, and garnet.

The Barnes Conglomerate Member grades upward into approximately 350 feet of interlayered quartzites and schists of the upper member of the Dripping Spring Quartzite. The upper Dripping Spring rocks crop out extensively along the crest of the mountains, and limited exposures are found in the Buehman Canyon region. These rocks have been intruded by numerous sills and dikes of diabase, but only the larger continuous masses have been mapped (Plate II).

Two distinct lithologic types make up the upper unit of the Dripping Spring Quartzite. The lower portion of the upper unit is characterized by abundant, light gray to pink quartzites with interbedded schists. The quartzites exhibit relict current cross-bedding, and occasionaly have what appear to be relict ripple marks. The schistose rocks which are intercalated with the quartzites and those which comprise the upper portion of the formation vary from light gray to reddish brown in color. Many of the schists exposed along the summit of the Catalinas have crumpled or crenulated foliation (Fig.4). The Dripping Spring Quartzite on the northeastern slope of Kellogg Mountain is extensively veined by aplitic to pegmatitic materials (Fig.5).

Thin section analysis of the quartzitic units within the upper Dripping Spring Quartzite shows the following minerals to be present: quartz, microcline, plagioclase, muscovite, biotite, epidote, and garnet. Quartz is the most abundant

mineral and makes up 55 to 85 per cent of the rock. The quartz grains range in diameter from 0.1 to 3.0 millimeter. Many of the larger grains display an internal mosaic texture, and all of the grains have sutured contacts to a greater or lessor extent. In the strongly recrystallized quartzites the grains are elongated in the plane of foliation and exhibit pronounced undulatory extinction. Microcline constitutes 5 to 30 per cent of the average rock (Fig. 6). The microcline crystals show the typical grid twinning and minor perthitic textures. The perthite develops in those rocks which have been intensively deformed and appears to fill tension cracks within individual grains, (Fig. 7). The wedge-shaped perthitic intergrowths make an acute angle with the planes of foliation and granulation in the surrounding materials. Oligoclase (An_{20-25}) accounts for 0 to 10 per cent of the quartzites. The plagioclase grains are often twinned according to the albite law, but many grains are untwinned. The feldspar content of the rocks indicates that they would more properly be termed feldspathic quartzites.

The micas occur as subhedral flakes which have parallel to subparallel orientations. The typical feldspathic quartzites contain less than 10 per cent mica. Locally they are richer in micas and hence grade into feldspathic schists. Muscovite is the most abundant mica and constitutes up to seven per cent of the rock. Biotite is present in smaller quantities and never exceeds five per cent. Subhedral to euhedral porphyroblasts of epidote are randomly scattered throughout the rock and comprise

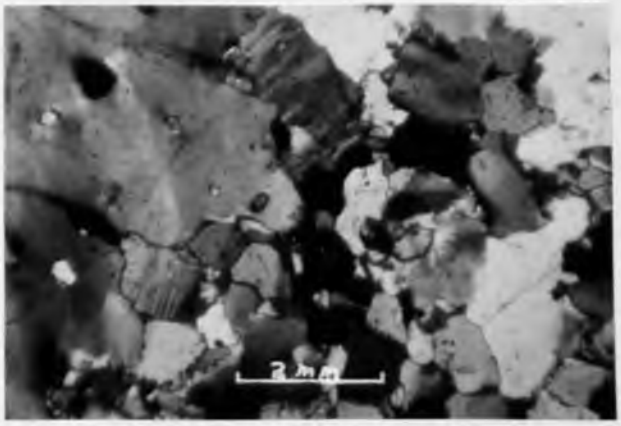

Figure 6. Photomicrograph of a feldspathic quartzite member of the upper Dripping Spring Quartzite exposed one mile east of Kellogg Mountain. Nicols crossed.

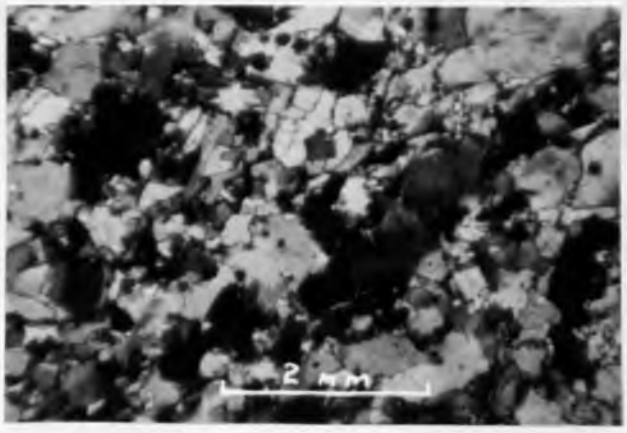

Figure 7. Perthite developed as wedge-shaped fillings in tension cracks within microcline grains found in the Dripping Spring Quartzite one-half mile east-southeast of Kellogg Mountain. Crossed Nicols.

two to five per cent of the volume. A few well-rounded detrital grains of epidote occur in the more quartzitic layers. Garnet is present in the more feldspathic quartzites near the summit of the range where it may make up as much as five per cent of the rock. The index of refraction, 1.817, and occurrence suggests that the composition is probably very similar to that found by the author for sample number Sc 286 (Pilkington, 1961).

Minor accessory minerals include rounded to sub-rounded relict detrital grains of zircon and magnetite. Leucoxene is not uncommon indicating that titanium bearing minerals were present. Apatite occurs as subhedral to euhedral grains.

Microscopically the feldspathic schists of the upper Dripping Spring Quartzite consist of quartz, plagioclase, microcline, muscovite, biotite, hornblende, epidote, and garnet. The minor minerals include magnetite, apatite, zircon, ilmenite, tourmaline, and sphene. Quartz constitutes 10 to 70 per cent of the rock. The quartz grains are strongly recrystallized and exhibit a rather distinct elongation in the rocks near the summit of the mountains (Fig. 8). However, the rocks exposed on the north side of Buehman Canyon are only weakly recrystallized (Fig. 9). The quartz grains range from 0.05 to 2.0 mm in diameter, with the average approximately 0.5 millimeter. Microcline occurs as anhedral crystals in the same size range as quartz. The potash feldspar comprises 10 to 50 per cent of the schists. Plagioclase (An_{20-25}) is present in amounts up to 15 per cent, but usually in the range of five per cent.

Muscovite or biotite compose 10 to 25 per cent of the feldspathic schists. In a given rock the mica will be predominantly one or the other type. Muscovite is found as subhedral flakes with parallel or subparallel orientation (Fig. 8). The grain size ranges from less than 0.1 to over 3.0 mm in length. Biotite occurs as subhedral flakes and also develops along the cleavages in muscovite grains. The typical biotite exhibits distinct pleochroism from dark brown to light tan. However, when it is found with hornblende the biotite is pleochroic in reddish-browns and tans. Hornblende as subhedral to euhedral crystals (Fig. 10) accounts for 0 to 15 per cent of certain layers in the schists. The hornblende varies from actinolitic hornblende, Z angle c equals 15^{o} and pleochroism from nearly colorless to pale green, to common green hornblende with extinction angles of 20 to 25 degrees and distinct pleochroism from pale green to dark green. Subhedral porphyroblasts of epidote up to one millimeter in diameter constitute two to ten per cent of the schistose rocks. Garnet occurs in minor amounts in some of the schistose rocks along the crest of the mountains. The garnets have a composition of alm_{52} sp_{23} $andr_{12}$ pyr_{13} as determined by the author (Pilkington, 1961).

Subhedral to euhedral crystals of apatite and magnetite are the most abundant and widespread of the accessory minerals. Both minerals tend to be more strongly concentrated along certain layers within the rocks. Zircon occurs as rounded to well-rounded relict detrital grains. A few tiny crystals of euhedral zircon appear as inclusions in quartz and feldspar grains.

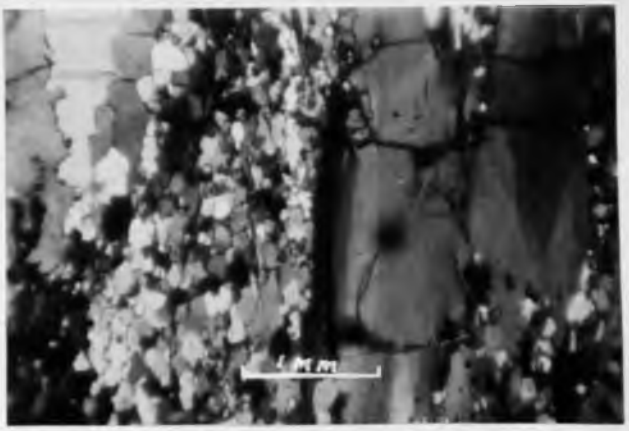

Figure 8. Strongly recrystallized quartz in a feldspathic schist of the Dripping Spring Quartzite on the north side of Kellogg Mountain. Nicols crossed.

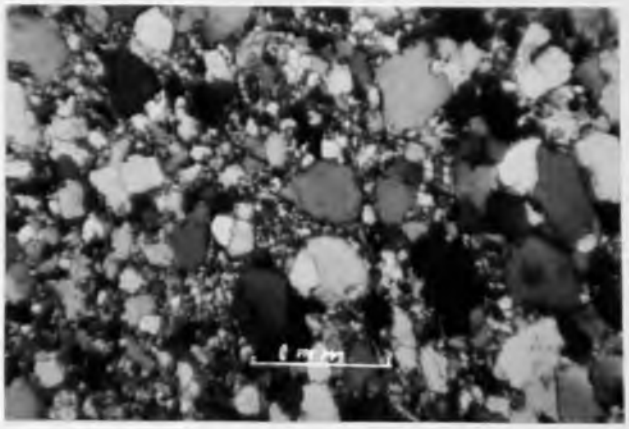

Figure 9. Photomicrograph of a weakly recrystallized unit in the upper part of the Dripping Spring Quartzite north of Buehman Canyon. Nicols crossed.

Tourmaline is common in certain layers of the schistose rocks and may make up as much as four per cent of the rock. The tourmaline occurs as subhedral to euhedral prisms up to 0.5 millimeters long, and is pleochroic from blue-green to pale green. The tourmaline probably belongs to the schorlite variety based upon its pleochroism.

The Dripping Spring Quartzite exposed in the eastern part of the area contains an abundance of calc-silicate material. Thin section study reveals the rocks consist of quartz, microcline, plagioclase, epidote, diopside, and garnet. The quartz content is exceedingly variable and ranges from less than five per cent up to forty per cent of the total volume. The quartz may be strongly recrystallized or only weakly recrystallized. The more strongly recrystallized material is found in the outcrops in the extreme southeastern part of the area. Minor amounts of microcline and plagioclase are present but usually constitute less than five per cent of the rock. Epidote is present as subhedral to euhedral porphyroblasts and may make up as much as 70 per cent of the given layer. Diopside represents a minor amount of the total volume in a few sections. Garnet is quite common and may comprise up to 10 per cent of the rock. The garnet is a mixture of almandine and grossularite.

The results of ten modal analyses for various units in the Dripping Spring Quartzite are shown in Table III. Each analysis represents 400 point counts made on a one millimeter

grid interval. The weight percentage of the various oxides calculated from the mode are given in Table IV.

The mineral composition, relict structures, and textural relationships found in the Dripping Spring Quartzite suggests that the original sediments were feldspathic sandstones and arkoses. The materials in the upper part of the section become increasingly finer grained, but still retain their feldspathic nature. The modal analyses (Table III) and chemical compositions (Table IV) compare closely with published analyses of feldspathic and arkosic sediments (for example, Pettijohn, 1957). The metamorphism resulted in some recrystallization of the feldspars and the formation of clear unaltered rims on the original detrital grains. Additional metamorphic minerals include: muscovite, biotite, hornblende, epidote, tourmaline, apatite, garnet, and magnetite. Locally the rocks exhibit the development of feldspar porphyroblasts for short distances away from the contacts with the banded augen gneiss. The spatial distribution and their fresh clear appearance suggests that the porphyroblasts formed as a result of metasomatism.

The origin of the atypical calc-silicate bearing Dripping Spring Quartzite deserves brief discussion. The areal distribution of the rocks in question suggests a metasomatic origin. The main area of calc-silicate development in the Dripping Spring Quartzite is found adjacent to the metamorphosed Paleozoic limestones in the Bullock Canyon area. Limited areas of calc-silicates are found adjacent to hydrothermal vein

Table III. Modal analyses of the Dripping Spring Quartzite.

Mineral	Sc 101	Sc 126	Sc 128	Sc 133	Sc 154
Quartz	45.2	44.8	37.2	59.9	29.9
Plagioclase	5.0	4.7	8.3	9.8	15.3
Microcline	25.3	10.3	10.1	19.7	34.8
Muscovite	19.7	29.6	1.7	6.8	--
Biotite	2.9	5.1	34.3	2.9	--
Epidote	1.8	1.7	2.0	--	5.7
Magnetite	0.7	1.1	1.6	1.1	1.3
Others	0.9	2.4	4.5	0.6	12.7**
	101.5	99.7	99.7	100.8	99.7

** Represents hornblende

Mineral	Sc 169	Sc 192	Sc 241	Sc 249	Sc 394
Quartz	40.1	45.1	75.1	74.1	62.2
Plagioclase	35.2	5.2	4.9	4.7	9.9
Microcline	9.8	9.9	11.3	11.8	20.3
Muscovite	6.7	29.7	7.8	4.9	1.7
Biotite	6.3	7.2	--	2.3	3.2
Epidote	--	--	--	--	--
Magnetite	0.8	1.3	0.9	1.8	1.1
Others	1.5	1.2	0.3	1.0	0.9
	100.4	99.6	100.3	100.6	99.3

Table IV. Chemical Compositions of the Dripping Spring Quartzite calculated from modal analyses.

Oxide	Sc 101	Sc 126	Sc 128	Sc 133	Sc 154
SiO	75.1	74.1	70.6	84.2	68.1
Al_2O_3	13.8	15.6	12.8	8.2	13.9
FeO	2.2	1.2	2.2	1.0	3.8
(Mg,Fe)O	0.6	0.7	5.8	1.3	0.8
CaO	0.7	0.2	1.7	0.2	4.8
Na_2O	0.5	0.5	0.5	0.4	1.2
K_2O	6.9	6.2	5.9	4.6	6.7
H_2O	0.7	1.4	0.9	0.4	0.1
	100.9	99.9	100.4	100.3	99.4

Oxide	Sc 169	Sc 192	Sc 241	Sc 249	Sc 394
SiO_2	74.9	72.1	89.2	88.7	83.9
Al_2O_3	14.3	15.6	6.8	6.0	7.9
FeO	1.0	1.1	--	1.1	1.0
(Mg,Fe)O	1.3	1.7	--	0.6	0.8
CaO	1.4	0.3	0.3	0.3	0.4
Na_2O	3.3	0.5	0.4	0.4	0.9
K_2O	3.3	6.3	2.9	2.9	4.2
H_2O	0.5	1.5	0.5	0.4	0.5
	100.0	99.1	100.1	100.4	99.6

fillings, which are found in the same vicinity, as well as a few which are located at some distance from the Paleozoic limestones. The source for the calcium appears to have been hydrothermal fluids, although minor amounts may have been derived from the limestones.

Mescal Limestone

The Mescal Limestone, the youngest formation of the Apache Group, crops out intermittently along the summit and northeastern slopes of the Catalina Mountains. The Mescal Limestone was found to conformably overlie the Dripping Spring Quartzite and to disconformably underlie the Bolsa Quartzite on the ridge northeast from Green Mountain. The limestone ranges in thickness from 0 to 20 feet. The rocks vary from light green to white on fresh surfaces and weather to a medium-gray. Lithologically the rocks change from rather pure carbonate in one layer to calc-silicates in the adjacent layers. The calc-silicates are more resistant to weathering and stand out as irregularities on weathered surfaces.

The purer carbonate layers consist of calcite, prochlorite, and penninite. Ninety to ninety-five per cent calcite is typical of the carbonate layers. The calcite is considerably recrystallized and elongated. Chlorite minerals make up the remainder of the rock and occur as scattered flakes and also as distinct layers parallel to the foliation within the carbonate. The penninite variety appears to replace the prochlorite.

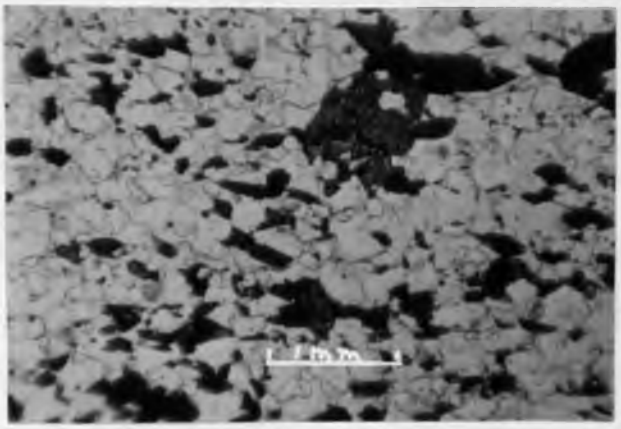

Figure 10. Photomicrograph of a hornblende-feldspar schist in the Dripping Spring Quartzite east of Nagge Peak. Plain light.

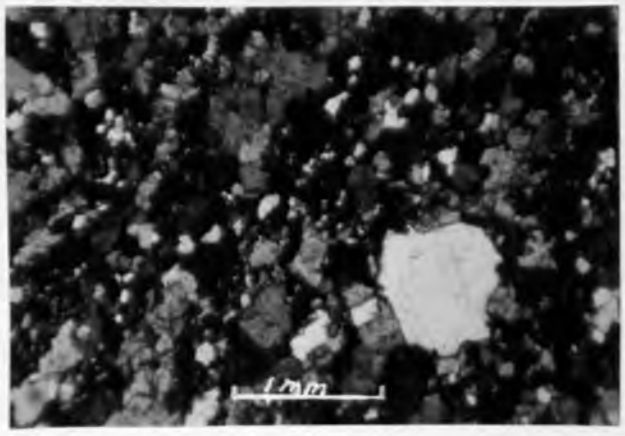

Figure 11. Weakly metamorphosed Mescal Limestone exposed along a tributary on the north side of Buehman Canyon. The light colored areas are quartz, the gray is calcite, and the black is epidote. Nicols crossed.

Optically the penninite variety displays the characteristic Berlin blue interference colors, is biaxial negative, and is length slow. The identification of the chlorite minerals was confirmed by means of X-ray diffraction. The weakly metamorphosed equivalents exposed north of Buehman Canyon are composed of calcite, quartz, and epidote (Fig. 11).

The calc-silicate layers are made up of calcite, tremolite, prochlorite, penninite, and minor amounts of diopside. Tremolite, present as subhedral crystals, accounts for 20 to 80 per cent of the calc-silicate layers. Chlorite minerals form 5 to 80 per cent of individual bands within the calc-silicate layers. Prochlorite is the most abundant chlorite mineral and usually makes up 90 or more per cent of the total chlorite. The penninite variety appears to replace the prochlorite.

Diabase

Dikes and sills of metamorphosed diabase are found within the Apache Group throughout the map area (Plate II). The diabase bodies vary considerably in thickness, and thicknesses of 30 to 50 feet are common. Several ages of diabase intrusion have been reported in the Catalina Mountains. Peirce (1958) reports that he observed diabase which intruded Cambrian rocks, and Moore and Tolman (1949) state that diabase bodies cut rocks as young as Cretaceous. During the present study the diabases were found only in rocks of the Apache Group, and for the lack of other criterion are considered to be equivalent to the Younger Pre-Cambrian diabases exposed elsewhere in southern Arizona.

The diabase is a dark green to blackish green amphibolitic rock. The diabase has been affected by the same grade of metamorphism as the country rock, and its foliation is parallel to that of the adjacent rocks. In the larger masses the central portion is considerably coarser-grained with a maximum grain size up to one centimeter. The chilled margins have retained their fine-grained texture. The rocks often contain stringers or pods of quartz and feldspar.

Thin section study shows the rocks to be composed of quartz, oligoclase, hornblende, biotite, and epidote. Accessory minerals include magnetite, apatite, sphene, and zircon. Quartz occurs in small amounts, usually less than five per cent. The quartz appears either as interstitial fillings or as poikiloblastic inclusions in the amphiboles. The interstitial quartz is often strained and exhibits moderate to strong undulatory extinction. The plagioclase (An_{20-25}) forms twinned or untwinned crystals which often retain the original subhedral to euhedral form. Subhedral to euhedral hornblende composes 15 to 40 per cent of the amphibolite (Fig. 13). The amphibole from the rocks exposed near the summit of the range is strongly pleochroic from brownish green to blue green, has a moderate 2V angle of approximately 50 degrees, and 20 degree extinction angles. The amphibolitic rocks in the Buehman Canyon area contain actinolitic hornblende which is pleochroic from pale green to light yellow, has a large 2V angle, and 17 degree extinction angles. The amphiboles occur as small euhedral prisms and as large crystalloblastic grains with abundant inclusions of quartz and plagioclase. Biotite occurs as

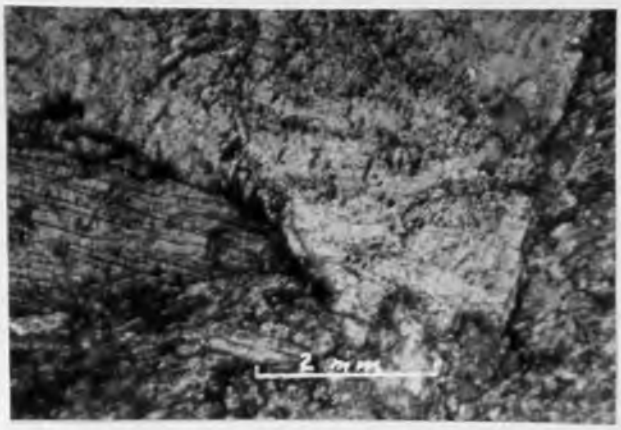

Figure 12. Photomicrograph of a calc-silicate layer in the metamorphosed Mescal Limestone. The large crystals are tremolite and are surrounded by chlorite. The rock is from the ridge northeast of Green Mountain. Nicols crossed.

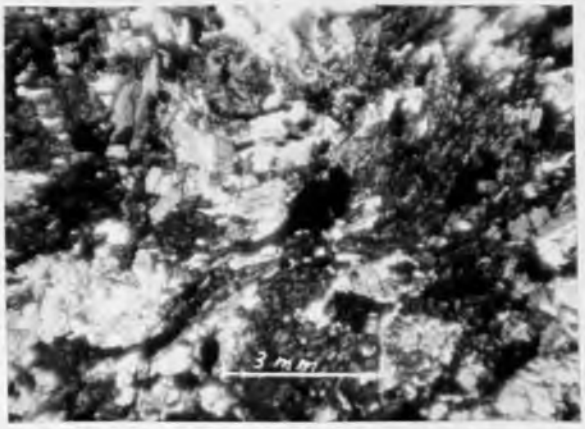

Figure 13. Amphibolite developed from the diabase body in the Dripping Spring Quartzite north of Kellogg Mountain. The dark areas are hornblende and the light areas are plagioclase. Plain light.

subhedral flakes which are intimately associated with epidote and secondary sphene. The quantity of biotite is small, but may be present in amounts up to 20 per cent. Epidote is found as porphyroblasts associated with the plagioclase grains and as anhedral secondary masses associated with biotite. Epidote comprises up to five per cent of the rock.

Subhedral to euhedral apatite crystals make up one to two per cent of the volume of the amphibolites. Magnetite and titano-magnetite is present in amounts equal to or greater than apatite. Sphene has two distinct habits. It appears as euhedral crystals disseminated throughout the rock and as anhedral masses associated with biotite and epidote formed by the destruction of original amphiboles or pyroxenes.

Paleozoic Rocks

Middle Cambrian

Bolsa Quartzite

The Bolsa Quartzite of Middle Cambrian age is the oldest Paleozoic rock exposed in the Santa Catalina Mountains. The quartzite rests disconformably upon either the Mescal Limestone or upon the Dripping Spring Quartzite of the Apache Group. The Bolsa forms a narrow band of exposures in the northwestern corner of the area studied (Plate II). The quartzite varies from white to light gray in color. It may be either massive or thin bedded and contains minor amounts of dark minerals and sericite along the bedding planes.

As determined microscopically the rocks are composed of quartz, muscovite, biotite, epidote, and diopside. A varied suite of minor minerals are present including zircon, sphene, magnetite, leucoxene, apatite, and rutile. Quartz is by far the most abundant mineral and makes up 70 to 95 per cent of the total rock. The grain size is extremely variable and diameters range from 0.5 to 8.0 millimeters. The quartz grains are distinctly elongated and the maximum diameter may be as much as five times the minimum diameter. The individual grains show strongly sutured contacts and moderate to strong undulatory extinction.

Muscovite constitutes 3 to 10 per cent of the rock and occurs as subhedral flakes which have a pronounced parallel orientation. The muscovite is fine-grained in most of the sections studied. Biotite is present in very minor amounts in a few specimens. Subhedral diopside crystals make up about 10 per cent of the quartzites exposed in the canyon east of Kellogg Mountain. Epidote occurs as subhedral grains which comprised one to five per cent of the rock.

The minor accessory minerals represent relict heavy minerals. Zircon, sphene, and rutile appear as rounded grains and each represents less than one per cent of the total volume. Magnetite occurs in amounts up to two per cent. Leucoxene is present as an alteration product of the original titanium bearing minerals.

Middle and Upper Cambrian

Abrigo Limestone

The Abrigo Limestone exposed within the area of investigation consists of 300 or more feet of metamorphosed argillaceous and calcareous sediments. The rocks have a sharp but conformable contact with the underlying Bolsa Quartzite. The distribution of the Abrigo Limestone is similar to that of the Bolsa (Plate II). Only the lower units are exposed in the area mapped. The upper units have been removed by erosion. The rocks of the Abrigo fall into two lithologic types. The original argillaceous layers have been converted into spotted schists while the calcaeous units have formed calc-silicate bands. The schistose rocks are silvery-gray to greenish-gray in color and contain knots or spots of dark green minerals. The calc-silicate layers typically consist of alternating white and light green bands.

The schistose rocks as observed petrographically consist of quartz, plagioclase, muscovite, biotite, chlorite, and epidote. Tourmaline, magnetite, apatite, and zircon are present as accessory minerals. Quartz composes 20 to 40 per cent of the schists. The quartz grains are xenoblastic and exhibit mutual contacts with minor suturing. The grain size averages 0.1 millimeter. Plagioclase (An_{20-25}) constitutes 10 to 30 per cent of the schistose layers. The oligoclase occurs as untwinned, subhedral crystals of the same size range as quartz.

Muscovite appears as small, subhedral flakes which have a very pronounced orientation and comprise 10 to 30 per cent of

the rock. The muscovite crystals wrap around the spots of dark minerals (Fig. 14). The muscovite grains within the spots are considerably larger than those of the matrix. Biotite forms as much as 15 per cent of the schist. It occurs as subhedral crystals and also forms along the cleavages of the muscovite grains. The biotite flakes have a much less rigorous orientation than do the muscovite flakes. Prochlorite as individual grains and as aggregates constitutes two to ten per cent of the volume. Epidote occurs in small quantities as porphyroblasts.

Pleochroic blue-green tourmaline appears as small prisms, less than 0.1 mm long, disseminated throughout the rock. The tourmaline, schorlite variety, averages two per cent of the schist. Magnetite is an equally abundant accessory mineral. Scattered, well-rounded relict detrital grains of zircon represent less than one per cent of the total volume. Apatite occurs as euhedral prisms with a random distribution.

The mineral composition of the calc-silicate layers within the lower Abrigo Limestone includes quartz, plagioclase, microcline, biotite, diopside-hedenbergite, hornblende, tremolite, tschermakite, vesuvianite, epidote, zoisite, and garnet. Minor minerals show much less variation and consist of sphene, zircon, apatite, and magnetite. Xenoblastic quartz makes up 5 to 50 per cent of the various layers. Plagioclase comprises 15 to 60 per cent of the calc-silicate rocks. The composition of the plagioclase is not everywhere the same. The An content ranges from

Figure 14. Spotted schist from the lower unit of the Abrigo Limestone northeast of Kellogg Mountain. The coarse-grained area in the center of the photograph represents one of the spots. Crossed Nicols.

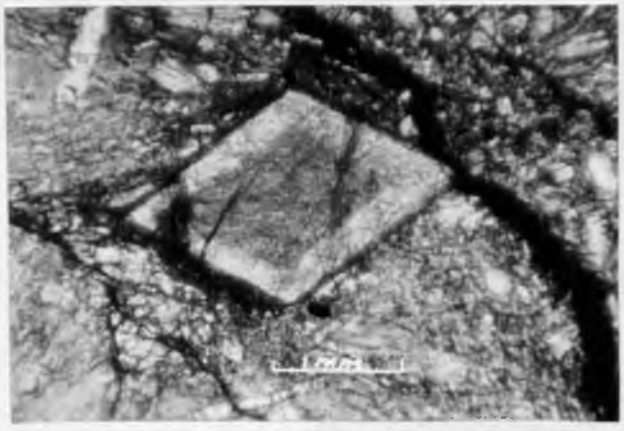

Figure 15. Photomicrograph of vesuvianite porphyroblast in a matrix of tschermakite from a calc-silicate layer in the Abrigo Limestone exposed northeast of Green Mountain. Nicols crossed.

20 to 65 and may be oligoclase in one layer and labradorite in the adjacent layer. The composition of the plagioclase was determined by the Michel Levy method whenever a sufficient number of twinned crystal were present. In the specimens containing untwinned plagioclase the material was separated from the rock and the composition determined by the Tsuboi method. Those rocks which have the higher concentrations of microcline contain the more calcic plagioclase. A more detailed discussion of the composition of the plagioclase will be given later. Anhedral microcline is commonly present in amounts from 10 to 50 per cent of the total volume.

Biotite associated with the calc-silicate rocks occurs in distinct bands and probably represents more argillaceous original layers within the calcareous units. The bands are thin and range from a few millimeters to several centimeters in thickness. Biotite may amount to ten per cent of an individual layer but constitutes only a small percentage of the entire rock. Idioblastic epidote and zoisite account for 5 to 40 per cent of the calc-silicate rocks. Euhedral porphyroblasts of vesuvianite (Fig. 15) constitute as much as 15 per cent of some of the calc-silicate layers.

Amphiboles of various compositions are present in amounts up to 70 per cent within certain of the calc-silicate layers. Common green hornblende occurs in many of the specimens studied. The hornblende is pleochroic from dark green to light green, has a 2V angle of approximately 60 degrees, and an extinction

angle of 22 degrees. The layers which contain the common green hornblende probably represent original aluminuous bands within the limestone. Tremolite is the amphibole found in many of the specimens studied and is believed to have formed from original dolomitic layers. Other calc-silicate layers were characterized by tschermakite; a colorless amphibole which has a moderate 2V angle of 45 degrees, N_y equaled 1.695, and an extinction angle of 19 degrees. The tschermakite formed from layers which were impure dolomites containing some iron, aluminum, and sodium.

Pyroxenes in the calc-silicate rocks are represented by both diopside and hedengergite (Fig. 16). The pyroxene content is exceedingly variable from one layer to the next and ranges from 5 to 95 per cent of the individual layers.

Subhedral to euhedral sphene is the most abundant minor mineral. Apatite is almost universal in its occurrence in the calc-silicate rocks, but never exceeds one per cent. Magnetite is present in most of the rocks and may equal the quantity of sphene.

Post-Paleozoic Rocks

Quartz Latite Porphyry

Dikes and irregular masses of metamorphosed quartz latite porphyry intrude the Paleozoic and Younger Precambrian rocks throughout the mapped area (Plate II). The thickness of the intrusive bodies ranges from a few feet to over 200 feet. The color varies from dark gray to buff on weathered surfaces

and is medium gray on fresh surfaces. The quartz latite is typified by the presence of doubly terminated quartz phenocrysts. Abundant oriented inclusions of metasedimentary rocks, which probably were derived from Pinal Schist, are common in the quartz latite porphyry.

Thin section examination reveals the blastoporphyritic rock to be composed of quartz, plagioclase, orthoclase, microcline, biotite, muscovite, and epidote. Minor accessory minerals found include apatite, zircon, sphene, and magnetite. Quartz occurs as relict phenocrysts up to four millimeters in diameter and also as anhedral grains about 0.05 mm in diameter in the groundmass. Quartz constitutes 10 to 25 per cent of the rock. A few of the quartz grains appear to be porphyroblastic. Plagioclase (An_{20-25}) in the form of relict phenocrysts (Fig. 17) and as anhedral grains in the groundmass comprises 25 to 40 per cent of the quartz latite. The plagioclase phenocrysts often show well developed relict oscillatory zoning. The majority of the plagioclase in the groundmass is untwinned, while twinning is present in all of the phenocrysts. Orthoclase appears as subhedral phenocrysts and as anhedral grains in the groundmass. The amount of orthoclase ranges from 25 to 35 per cent. Microcline replaces some of the plagioclase phenocrysts and also has formed from orthoclase crystals in the groundmass.

Biotite is present as subhedral flakes whose parallel orientation accounts for the schistosity of the rock. Biotite makes up 5 to 15 per cent of the quartz latite. It is often

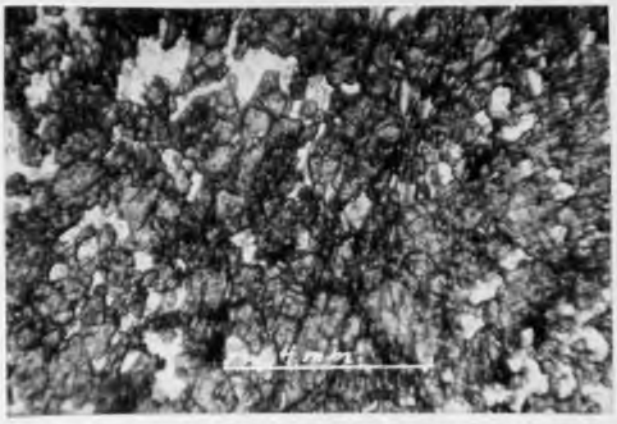

Figure 16. Photomicrograph of hedenbergite, the gray areas, and zoisite (the dark gray areas) in the Abrigo Limestone northeast of Green Mountain. Nicols crossed.

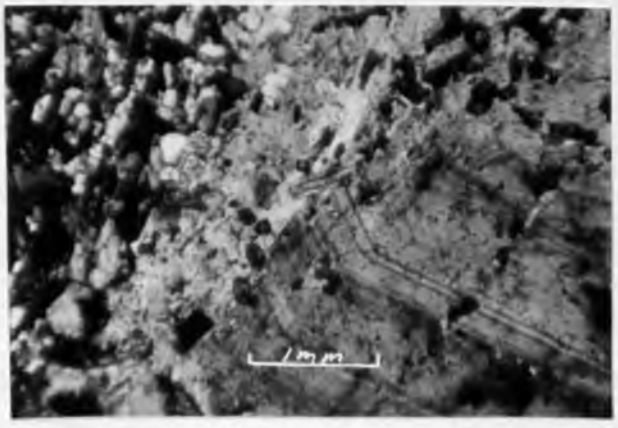

Figure 17. Metamorphosed quartz latite porphyry with oscillatory zoned plagioclase phenocryst in a fine-grained matrix, with porphyroblasts of muscovite. Crossed Nicols.

intimately associated with epidote and magnetite which suggests that the biotite was derived from earlier amphiboles. Subhedral to anhedral porphyroblasts of muscovite constitute three to five per cent of the rock. The muscovite occurs within the plagioclase phenocrysts and also within the groundmass. Subhedral to euhedral porphyroblasts of epidote and the anhedral epidote associated with biotite comprise 5 to 10 per cent of the total volume.

Sphene and apatite are the most abundant accessory minerals. Subhedral magnetite is present in slightly smaller quantities, usually less than one per cent. Zircon is present only in trace amounts and occurs as inclusions in feldspars and quartz.

Catalina Gneiss

The majority of rocks exposed in the southern half of the area investigated are Catalina Gneiss. The gneissic rocks were subdivided by DuBois (1959) into three general types, but all gradations exist between the different types. The divisions of the Catalina Gneiss include: banded augen gneiss, granitic augen gneiss, and granitic gneiss. The contact between the banded augen gneiss and the granitic gneiss was mapped (Plate II); however, no attempt was made to distinguish between the granitic augen gneiss and the granitic gneiss. Such a distinction has to be one based upon fabric, as will be discussed later. The granitic gneiss forms the core of the gneissic complex and the banded augen gneiss is found along the flanks.

Banded Augen Gneiss

The banded augen gneiss along the northeastern slopes of the Catalina Mountains is characterized by wavy foliation (Fig. 18). The augen consist of porphyroblasts of quartz and feldspar up to an inch or more in diameter. The rocks weather to various shades of gray or yellow-brown depending upon the oxidation state of the iron. The banded augen gneiss exhibits gradational contacts with the granitic gneisses over distances of a few inches up to a foot or more (Fig. 19). Numerous aplitic to pegmatitic bodies are found in the porphyroblastic augen gneisses which are in close proximity to the granitic gneiss (Fig. 20 and 21). The banded augen gneiss contains numerous inclusions of incompletely feldspathized metasedimentary rocks.

As observed microscopically quartz appears as small anhedral grains in the matrix and as augen porphyroblasts up to 10 mm in diameter. Many of the augen show a pronounced mortar structure. In a few of the rocks the quartz in the matrix has recrystallized to form lenticular stringers. Quartz comprises 25 to 60 per cent of the gneissic rocks. Plagioclase occurs as xenoblastic to idioblastic crystals in the groundmass and as subhedral porphyroblasts. The oligoclase (An_{20-25}) may be twinned or untwinned and constitutes 10 to 35 per cent of the rock. The boundaries between quartz and plagioclase often form myrmekitic intergrowths. The feldspar crystals, especially the porphyroblasts, contain abundant poikiloblastic inclusions of quartz. The plagioclase exhibits slight to moderate sericitic

Figure 18. Wavy foliation in the porphyroblastic banded augen gneiss southeast of Maverick Peak. Photograph of a nearly vertical face looking to the northeast.

Figure 19. Granitic gneiss which contains stringers of banded augen gneiss. Photograph of an outcrop east of Maverick Peak near the contact between the banded augen gneiss and the granitic gneiss.

Figure 20. Banded augen gneiss cut by numerous aplitic and pegmatitic bodies on the north slope of Green Mountain. Photograph taken from the Brush Corral trail looking to the southwest.

Figure 21. Replacement bodies of aplitic materials in the banded augen gneiss on the south side of Maverick Peak. A vertical face observed from the southwest.

alteration. Potash feldspar accounts for 15 to 40 per cent of the gneiss. The alkali feldspar occurs as subhedral to anhedral masses in the groundmass and also as idioblastic porphyroblasts up to eight millimeters in diameter. Two distinct varieties were found petrographically. The most abundant form is slightly perthitic microcline; however, a considerable amount of finely twinned or untwinned potash feldspar with a moderate 2V angle of 45 to 55 degrees is present. X-ray diffraction indicates that the second potash feldspar is orthoclase and its significance will be discussed in more detail in the section on petrogenesis. The feldspar with anomalous optical properties is believed to represent submicroscopic intergrowths of microcline and orthoclase. The anomalous potash feldspar occurs as discrete grains in the matrix and as irregular masses replacing the plagioclase porphyroblasts.

Biotite appears as subparallel flakes and composes 5 to 15 per cent of the entire rock. The biotite-rich layers wrap around the porphyroblasts to give the rock its distinctive wavy foliation. The mica is strongly pleochroic, from dark brown to yellow-brown. Muscovite forms subhedral flakes in the micaceous layers and subhedral porphyroblasts in the plagioclase crystals. The muscovite content is extremely variable, but always less than the biotite. Small quantities of epidote are present. Euhedral garnets, usually less than one millimeter in diameter, are found in the banded augen gneisses adjacent to the aplitic and pegmatitic masses. The composition of the garnets

is alm_{34} sp_{49} pyr_8 $andr_9$ (Pilkington, 1961).

Apatite is a common minor mineral found within the biotite-rich layers of the banded augen gneiss. Zircon occurs as tiny euhedral inclusions in quartz and feldspar grains, and also as scattered well-rounded, somewhat cloudy, relict detrital grains. Subhedral to anhedral magnetite is a common minor constituent. Sphene occasionally appears in thin sections of the banded augen gneiss.

The metasedimentary inclusions found within the banded augen gneiss are composed of quartz, microcline, plagioclase, muscovite, biotite, and minor amounts of apatite, magnetite, and epidote. Anhedral quartz grains compose 40 to 45 per cent of the inclusions. The quartz is recrystallized and shows moderate to strong undulatory extinction. Very fine-grained micas form the matrix in which the quartz grains are dispersed. Muscovite is the most abundant mica; however, small quantities of biotite are always present. Microcline may comprise up to 10 per cent, and appear to represent relict detrital grains. Oligoclase as clear untwinned grains may make up as much as five per cent of the rock.

Modal analyses, based upon 350 point counts, and the chemical compositions computed from them are shown in Table V and Table VI respectively. The discussion of the original materials from which the banded augen gneisses were derived will be given in the section on petrology.

Table V. Modal analyses of the banded augen gneiss.

Mineral	Sc 190	Sc 200	Sc 269	Dv 288	Sc 463
Quartz	25.1	39.7	39.9	28.6	44.7
Plagioclase	19.9	26.1	10.2	19.2	9.8
Microcline	40.3	14.9	30.4	34.3	30.3
Muscovite	3.9	9.2	5.7	1.7	4.3
Biotite	6.3	6.2	10.2	14.1	7.1
Epidote	1.8	2.3	2.9	0.6	2.1
Magnetite	1.1	0.9	0.9	1.1	0.7
Others	1.2	0.6	0.4	1.3	0.7
	99.6	99.9	100.6	100.9	99.7

Table VI. Chemical compositions calculated from the modal analyses.

Oxide	Sc 190	Sc 200	Sc 269	Sc 288	Sc 463
SiO_2	69.2	70.4	74.0	71.5	74.7
Al_2O_3	15.8	15.3	13.3	13.9	12.8
FeO	2.4	1.2	1.4	1.2	1.4
(Mg,Fe)O	1.0	1.3	1.9	2.9	1.3
CaO	1.5	2.5	1.1	1.3	1.1
Na_2O	1.1	3.1	2.9	3.8	2.9
K_2O	7.9	5.5	4.9	5.9	6.3
H_2O	0.9	0.6	0.5	0.5	0.8
	99.8	99.9	100.0	101.0	101.3

Granitic Gneiss

Granitic gneiss represents the most abundant rock type in the southern half of the region (Plate II). Texturally, the rocks grade from weakly deformed granitic gneisses through various stages of augen gneisses and finally into mylonitic rocks. The gneissic texture results from parallel alignment of micas which has been enhanced by cataclastic deformation of feldspars, quartz, and micas in many of the rocks. The medium-grained granitic gneiss varies from buff to yellow-brown on weathered surfaces and is light gray when freshly broken. The rocks are usually quite massive in outcrop. Replacement pegmatites and aplites are common.

Thin section investigation shows that the granitic gneiss has a remarkably uniform mineralogical composition. The major rock forming minerals are quartz, plagioclase, potash feldspar, muscovite, biotite, epidote, and garnet. Minor quantities of magnetite, apatite, and zircon are present. Quartz ranges from 20 to 35 per cent of the rock and averages approximately 30 per cent. The quartz occurs as porphyroclasts, irregular interstitial masses, finely granulated aggregates in the matrix of mylonites, and as recrystallized stringers. In the deformed rocks the quartz has moderate to strong undulatory extinction and shows considerable elongation. Myrmekitic intergrowths with plagioclase are common. The crystalloblastic fabric of the granitic gneiss is well exemplified by the feldspars and quartz (Fig. 22). Oligoclase (An_{20-25}) comprises 20 to 40 per cent of the granite gneiss;

Figure 22. Photomicrograph illustrating the crystalloblastic fabric of the granitic gneiss found near Rose Canyon Lake. Nicols crossed.

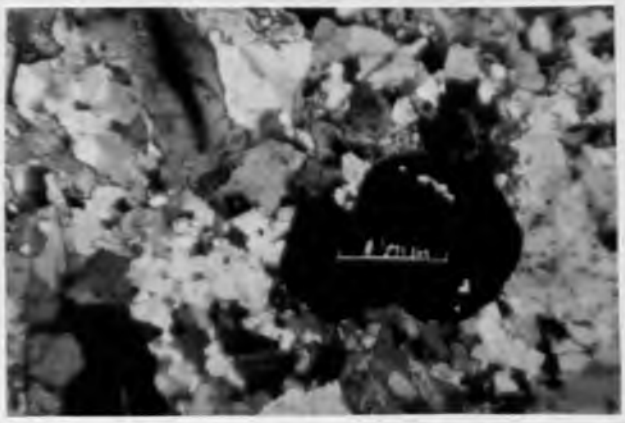

Figure 23. Typical crystalloblastic fabric of the aplitic materials found in the banded augen gneiss on Green Mountain. A large garnet crystal appears in the central portion. Crossed Nicols.

the average content is about 30 per cent. Many of the crystals exhibit relict normal progressive zoning. The plagioclase always show weak sericitic alteration and may contain oriented plates of muscovite. Poikiloblastic inclusions of quartz are common. Myrmekitic intergrowths are well developed in the cataclastically deformed rocks. The potassium feldspar content of the granitic gneiss averages 30 per cent and ranges from 20 to 35 per cent. Two distinct varieties of alkali feldspar are present. The most abundant one is microcline which occurs as anhedral to subhedral, somewhat perthitic, crystals. The perthite is best developed in areas of intense deformation. The second potash feldspar occurs as anhedral interstitial masses and as replacements of plagioclase feldspars. It is characterized by faint grid twinning or as untwinned individuals which have a moderate 2V angle of 45 to 55 degrees as determined by universal stage techniques. Optically the second feldspar falls between orthoclase and microcline, and is believed to represent a submicroscopic intergrowth of the two types. The relationships will be discussed in more detail later. The grain size ranges from finely granulated aggregates to porphyroblasts 10 mm or more in diameter. Poikiloblastic inclusions of quartz, plagioclase, and biotite are common in the potash feldspar porphyroblasts.

Muscovite is the most abundant mica and occurs as subhedral flakes which wrap around the porphyroblasts. In the strongly deformed rocks the micas are often streaked out. Muscovite commonly occurs as symplectitic intergrowths with quartz.

Muscovite makes up from 2 to 10 per cent of the gneiss and averages nearly 10 per cent. Biotite comprises approximately five per cent of the rock. Euhedral, anhedral, or granulated garnet crystals constitute a small but very characteristic part of the granitic gneiss. The average composition of the garnets is alm_{47} sp_{31} pyr_{10} $andr_{12}$ (Pilkington, 1961). The garnet crystals may contain abundant inclusions or may be free of inclusions. A few epidote phorphyroblasts are commonly present.

Anhedral to euhedral apatite is the most widespread of all the accessory minerals. The apatite grains range from prisms 0.01 mm or less to anhedral masses as much as 0.5 mm in diameter. Zircon appears as very tiny euhedral inclusions in quartz and feldspar. Scattered throughout the rock are larger, somewhat rounded zircon grains which probably are relict minerals. Magnetite in various stages of oxidation is the only other minor mineral.

Table VII shows the results of ten modal analyses of the granitic gneiss. Each modal analysis is based upon 250 point counts. The chemical compositions determined from the modes are given in Table VIII. The nature of the original materials from which the granitic gneiss was derived will be discussed in the section on petrology.

Table VII. Modal analyses of the granitic gneisses.

Mineral	Sc 139	Sc 147	Sc 156	Sc 206	Sc 217
Quartz	34.1	24.9	19.8	29.8	30.1
Plagioclase	19.8	30.1	39.6	30.2	24.6
Microcline	29.2	30.2	20.1	24.7	29.8
Muscovite	6.8	6.2	8.2	8.8	5.9
Biotite	5.1	6.3	5.9	--	3.9
Epidote	0.8	--	1.8	1.9	1.7
Magnetite	1.1	--	1.2	1.0	1.2
Others	2.3	2.3	3.0	3.1	2.7
	99.2	100.0	99.6	99.5	99.9

Mineral	Sc 257	Sc 290	Sc 330	Sc 357	Sc 473
Quartz	24.8	29.6	28.2	29.3	30.1
Plagioclase	34.6	25.2	26.4	34.6	25.5
Microcline	25.2	29.7	30.5	25.3	29.6
Muscovite	7.6	6.9	7.2	7.1	8.4
Biotite	4.7	4.4	4.9	--	2.7
Epidote	--	2.1	1.7	2.2	2.3
Magnetite	1.9	0.9	1.5	1.8	0.7
Others	1.2	1.0	--	--	1.4
	100.0	99.8	100.4	100.3	100.7

Table VIII. Chemical compositions of the granitic gneiss calculated from modal analyses.

Oxide	Sc 139	Sc 147	Sc 156	Sc 206	Sc 217
SiO_2	73.2	69.7	66.5	70.6	68.1
Al_2O_3	14.5	15.8	18.7	15.8	18.6
FeO	1.3	2.2	1.3	1.4	1.3
(Mg,Fe)O	1.0	1.3	1.2	1.3	1.0
CaO	1.3	1.2	2.1	1.7	1.5
Na_2O	2.9	3.3	4.1	3.2	3.8
K_2O	5.5	6.2	5.5	5.2	5.1
H_2O	0.5	0.5	0.6	0.5	0.4
	100.2	100.2	100.0	99.7	99.8

Oxide	Sc 257	Sc 290	Sc 330	Sc 357	Sc 473
SiO_2	69.2	71.4	70.4	69.1	68.2
Al_2O_3	17.0	15.7	15.8	16.0	17.3
FeO	2.0	1.3	1.4	2.3	1.3
(Mg,Fe)O	1.0	0.8	0.9	1.4	1.0
CaO	1.4	1.6	1.6	1.4	1.5
Na_2O	3.3	3.4	3.8	3.3	3.7
K_2O	5.8	5.5	5.6	6.2	6.1
H_2O	0.5	0.4	0.6	0.5	0.4
	100.2	100.1	100.1	100.2	99.5

Aplites and Pegmatites

Aplitic to pegmatitic dikes, sills, and irregular masses are found within the Younger Precambrian metasediments, the lower Paleozoic rocks, and in the Catalina Gneiss (Fig. 5, 20, and 21). Many of these granitic masses contain relict structures parallel to those in the country rock. The number of exposures decreases rapidly northeastward from the summit of the mountains and these rocks disappear within two miles. Texturally, the individual bodies vary from aplitic to pegmatitic with no apparent relationship to the country rock contacts. The contacts may be sharp or gradational and usually change in nature along the strike of a given mass.

The aplitic and pegmatitic rocks exhibit a granoblastic texture (Fig. 23) and are composed of quartz, plagioclase, potash feldspar, muscovite, biotite, and garnet. Twenty to forty per cent of the rock is made up of quartz. The grains are extremely irregular in outline as a result of deformation and recrystallization. Subhedral to anhedral plagioclase (An_{20-25}) constitutes 25 to 40 per cent of the granitic rocks. The plagioclase crystals are often broken and appear to swim in a matrix of potassium feldspar. The potassium feldspars comprise 25 to 55 per cent of the rock and two types can be distinguished under the microscope. Microcline appears as relict grains which exhibit the same degree of deformation as the plagioclase crystals. The second variety is characterized by very faint grid twinning, if any, and a 2V angle of 45 to 55 degrees.

X-ray diffraction results indicate that such feldspars represent an intergrowth of microcline and orthoclase. The second type of potash feldspar occurs interstitial to all other minerals.

Post-Cretaceous Rocks (?)

Quartz Latite (?)

Two post-metamorphic dikes of a very fine-grained leucocratic rock occur in the northeastern part of the area (Plate II). The vertical dikes intrude the metamorphosed quartz latite porphyry previously discussed, and the Pioneer Formation of the Apache Group. The age designation is uncertain and the rocks are placed here to conform with the age designations used by Peirce (1958) and Moore and Tolman (1949) for similar dike rocks.

The leucocratic dike rocks consist of phenocrysts of quartz and oligoclase (An_{18-22}) in a fine-grained groundmass of potash feldspar (?), plagioclase, and quartz. Deuteric or hydrothermal alteration of the plagioclase resulted in extensive sericite formation. Minor minerals present are apatite and zircon.

Andesite Porphyry

Several small dikes of post-metamorphic andesite porphyry intrude the Younger Precambrian rocks and the granitic gneisses in the west-central portion of the area mapped. The small size and limited lateral extent of the intrusives prevented showing them on the geologic map. The thickness of the dikes ranges

from less than one foot a maximum of three feet. The lateral extent of the dikes was difficult to determine because of the heavy cover, and none were traced more than 200 feet along their strike. The rock is yellow-green to greenish-brown on weathered surfaces and a medium gray on freshly broken rocks.

Petrographic investigation reveals that less than five per cent quartz occurs as anhedral grains in the fine-grained groundmass. Approximately 65 per cent of the andesite consists of plagioclase with an anorthite content of 40 per cent. The andesine phenocrysts often exhibit zoning. Hornblende represents the mafic constituent and forms 15 per cent of the rock. Many of the hornblende phenocrysts are zoned and some are twinned. Euhedral sphene crystals are disseminated throughout the groundmass. Deuteric or hydrothermal alteration resulted in the development of biotite and epidote at the expense of hornblende and sericite from the plagioclase.

Small dikes of andesite porphyry which display a "turkey track" texture (Cooper, 1961) intrude the granitic gneiss and Apache Group in the southeastern corner of the area. The limited extent of the outcrops necessitated that they not be depicted on the geologic map. The rock is dark gray to black in color. Phenocrysts of plagioclase up to one inch in length show no preferred orientation.

Thin section analysis indicates that plagioclase in the calcic andesine (An_{45-50}) range comprises 70 to 80 per cent of

the volume. The plagioclase occurs as euhedral phenocrysts with minor zoning and which contain inclusions of pyroxene. The plagioclase of the matrix appears as subhedral grains. Small phenocrysts of augite and hypersthene account for 5 to 10 per cent of the andesite. Other minerals which are present include quartz and potash feldspar. Late magmatic or deuteric alteration formed bowlingite at the expense of hypersthene and olivine.

STRUCTURE

The major structural features of the Santa Catalina Mountains are shown on Plate I. The area of the present investigation lies on the northeastern flank of the major dome. The structural details within the map area are shown on Plates II and III. Several minor folds along the flank of the dome were mapped in the current study. Many minor dislocations were observed, but only two large faults were mapped. Detailed observations were made on the foliation, lineation, and jointing.

Faults

The largest fault trends west-northwest across the northern part of the area and represents the eastward continuation of a fault mapped by Peirce (1958). The fault is nearly vertical and the south block moved downward. The stratigraphic throw increases to the west where the Bolsa Quartzite is in contact with the Pioneer Formation of the Apache Group.

In the northwestern portion of the area a steeply dipping reverse fault can be traced approximately two miles. The stratigraphic throw is such that the Dripping Spring Quartzite is brought into contact with the lower Abrigo Limestone.

A small fault breccia zone occurs in the Catalina Gneiss along the Mount Lemmon highway one-quarter of a mile south of the Catalina Trailer Park. The breccia zone strikes N65E and dips 45 degrees to the north. The fault cuts the aplitic and

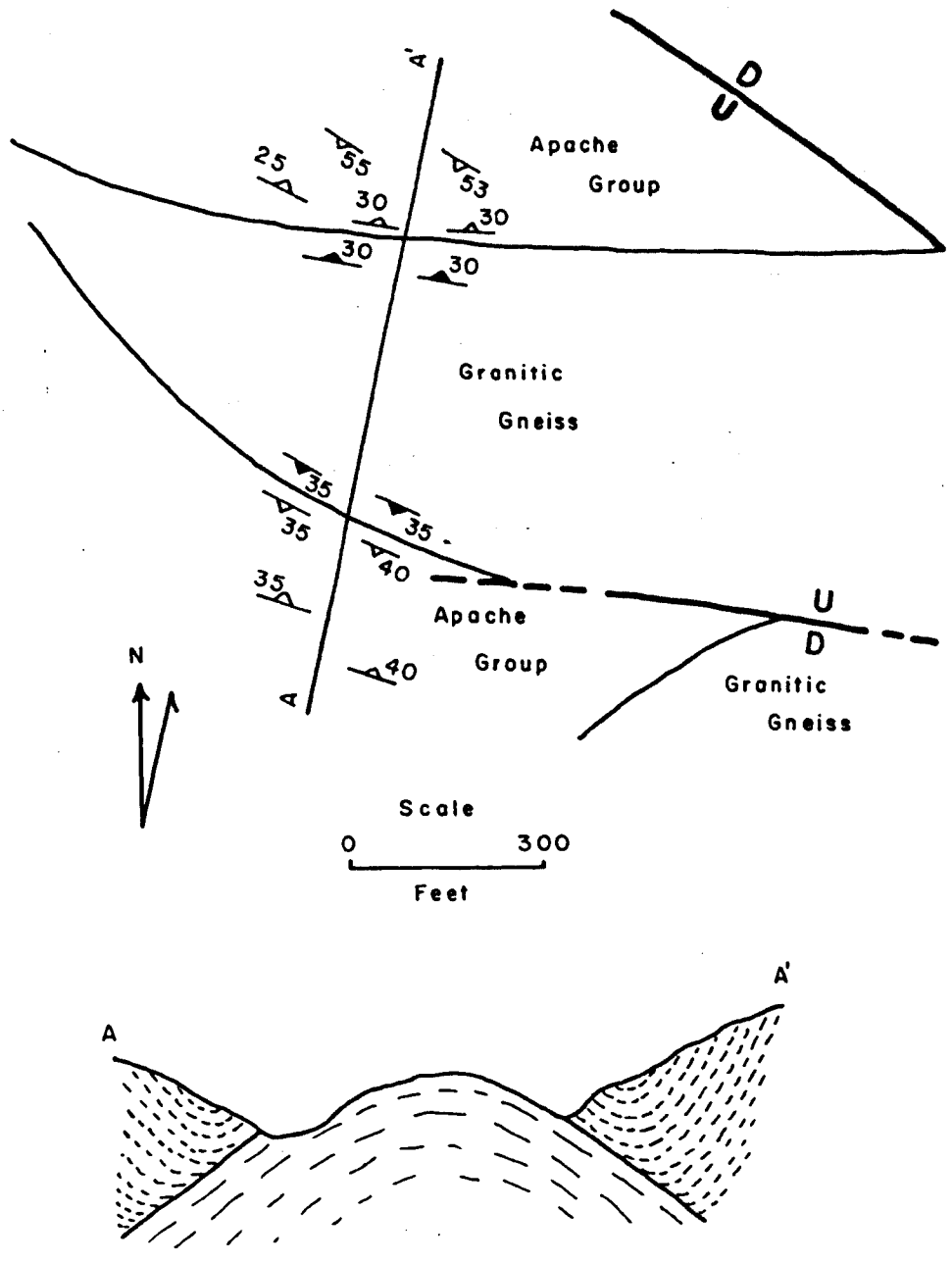

Figure 24. Sketch map of a small area one-half mile east of Kellogg Mountain with a cross-section to show the structural relationships.

pegmatitic bodies as well as the gneissic rocks. Another minor fault is exposed one-half mile east of Kellogg Mountain. The fault strikes N85W and dips 57 degrees to the south. The fault zone is intensely silicified and contains minor amounts of copper mineralization (Fig. 24).

Folds

The northeast flank of the large dome which makes up the Santa Catalina Mountains has numerous minor folds on it. The folds range in size from those a mile or more in width and several miles long, down to micro-folds found in the schistose rocks of the Apache Group. A large synclinal structure is present in the Apache metasediments located between the reverse fault, described above, and the granitic gneisses of the core of the mountains (Plate II). The fold axis strikes west-northwest. The asymmetrical syncline dips gently on the southwest flank and steeply on the northeast side.

In the central part of the area the foliation within the banded augen gneiss and the granitic gneiss outlines a series of anticlines and synclines. The fold axes trend west-northwest parallel to the major dome. One-half mile east of Kellogg Mountain small folds were formed when the granitic gneiss was intruded. The fold axes parallel the contact and are shown schematically in Figure 24.

The lower units of the Apache Group which crop out near the summit of the range contain numerous small drag folds which are asymmetrical toward the axis of the main dome. The drag folds are small, usually less than ten feet across, and traceable only for short distances along their strike because of the heavy cover. The axes of such folds strike N70W to N80W with few exceptions. The largest concentration of drag folds are located on the slopes of Kellogg Mountain. Small ptygmatic folds are common in the Pioneer and Dripping Spring metasediments when they crop out adjacent to the granitic gneiss.

The foliation of the Apache Group near the crest of the range is characterized by crenulation or crinkling. The microfolds responsible for the irregularities are most abundant in the outcrops near Kellogg Mountain and those northeast of Green Mountain. The most common type are flexural-slip folds which formed as a result of flexure and slippage along planes parallel to the axial plane (Fig. 25 and 26). However, numerous examples of chevron and accordion folds were observed.

Foliation

The gneissic rocks of the core and the metasedimentary rocks along its flank in the Santa Catalina Mountains all exhibit foliation (planar parallelism). In general the foliation strikes west-northwest and dips to the northeast within the area of this investigation. Several different foliate structures are present

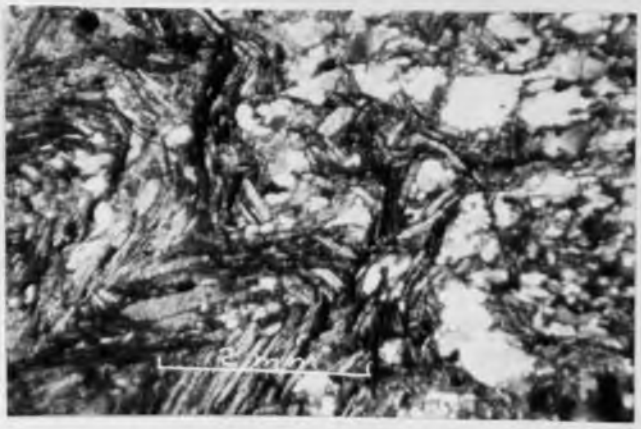

Figure 25. Flexural-slip folds in the upper Dripping Spring Quartzite exposed northeast of Kellogg Mountain. Nicols crossed.

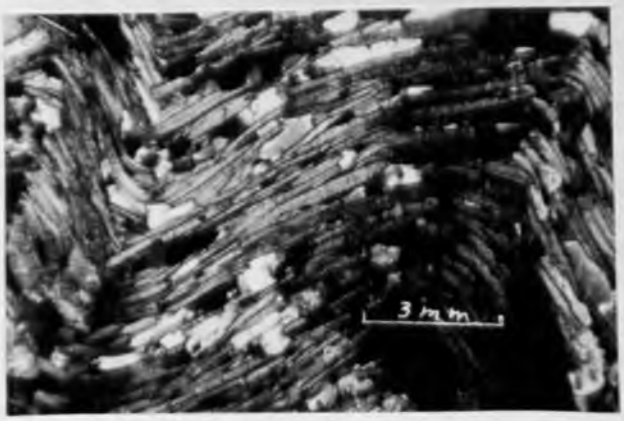

Figure 26. Flexural-slip folds in the Dripping Spring Quartzite east of Green Mountain. Nicols crossed.

in the rocks. In the following discussion the foliation has been classified according to the s-surface concept of Sander (1930). A schematic diagram which illustrates the relationships of the various s-surfaces is given in Figure 27.

S_1-surface

The oldest recognizable foliate structure within the area occurs in the banded augen gneiss exposed along the southern side of Buehman Canyon. The gneissic rocks are overlain by various members of the Pioneer Formation (Plate II). The s_1-surface represents the relict foliation preserved along the immediate vicinity of the contact (Fig. 28). The relict foliation strikes N65W and dips 50 degrees to the southwest and is characterized by both planar parallelism of minerals and by mineralogical banding. The foliation in the overlying Pioneer rocks strikes N65W and dips 55 degrees to the northeast. The contact between the banded augen gneiss and the rocks of the Apache Group is an extremely irregular surface which probably represents surface irregularities developed on the upturned rocks prior to the deposition of the Apache Group. The s_1-surface is only locally preserved and was destroyed elsewhere by the development of the s_2-surfaces.

S_2-surfaces

The most conspicuous foliation found in the rocks of this study is related to the s_2-surfaces. The foliation is

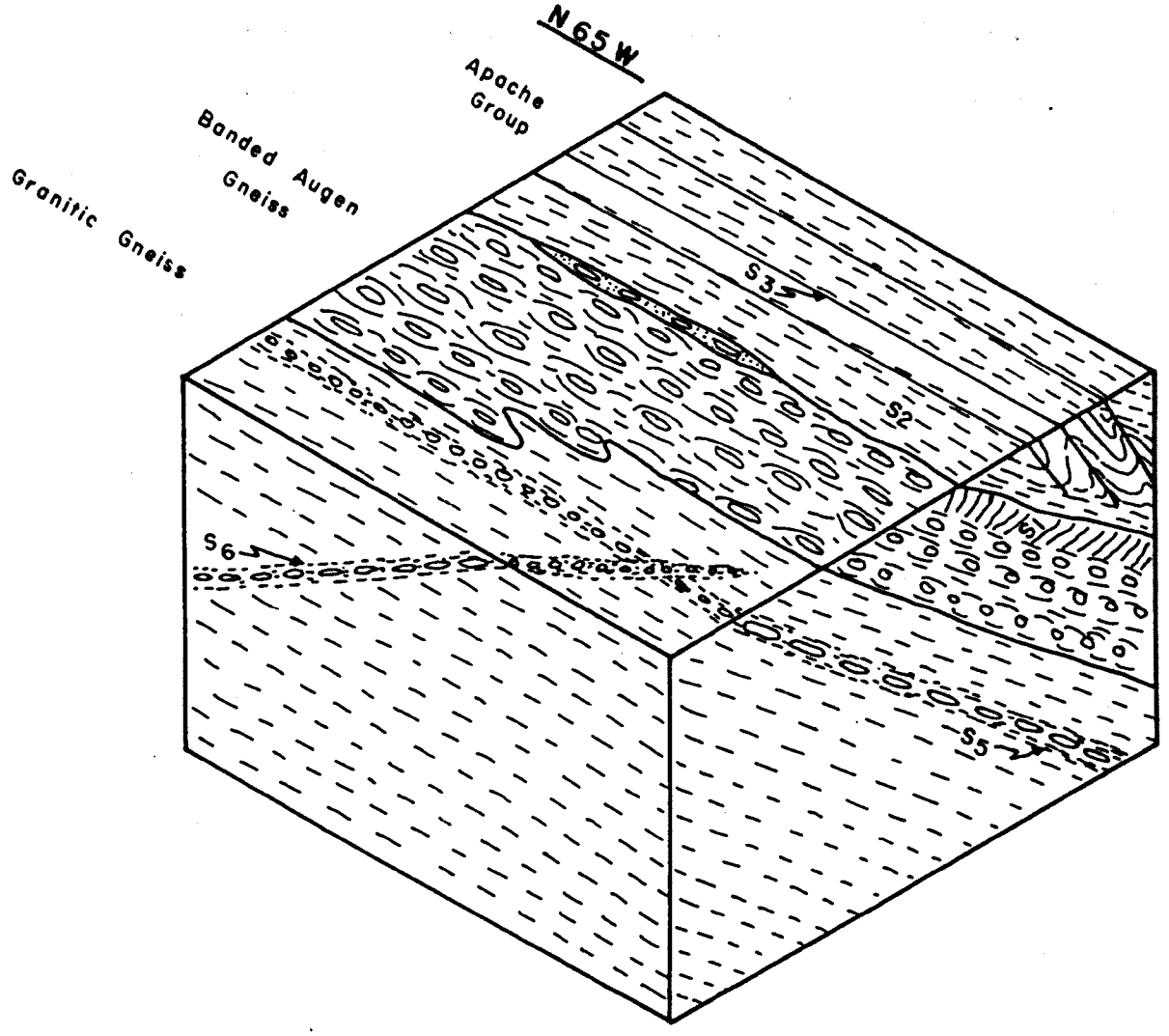

Figure 27. Block diagram to illustrate the relationships between the various s-surfaces found along the eastern flank of the Santa Catalina Mountains.

developed in both the gneissic rocks and the metasedimentary rocks (Plate II). In the metamorphosed sediments the s_2-surface may be regarded as essentially parallel to the original bedding. For example, the foliation within different lithologic units such as the Barnes Conglomerate is parallel with the foliation in the quartz-mica schists of the underlying Pioneer Formation and also with that in the overlying feldspathic quartzites of the upper Dripping Spring Quartzite Member. On a microscopic scale the s_2-surfaces in the Apache Group are shown by alternating layers of quartz and feldspar with mica-rich layers (Fig. 25). With the exception of the locally preserved s_1-surfaces the foliation of the banded augen gneiss coincided with s_2-surfaces described above. As shown in Figure 28 s_2-planes are also present in those banded augen gneisses which show the s_1-surfaces.

The granitic gneiss exposed in the southeastern part of the area exhibit well developed s_2-surfaces (Fig. 29) which are parallel to the foliation of the banded augen gneiss. The granitic gneisses of the south-central and western portions all show s_2-surfaces which have been modified to a greater or lesser extent by later deformation.

S_3-surfaces

The s_3-surface is represented by the axial plane foliation in the rocks of the Apache Group exposed near the crest of

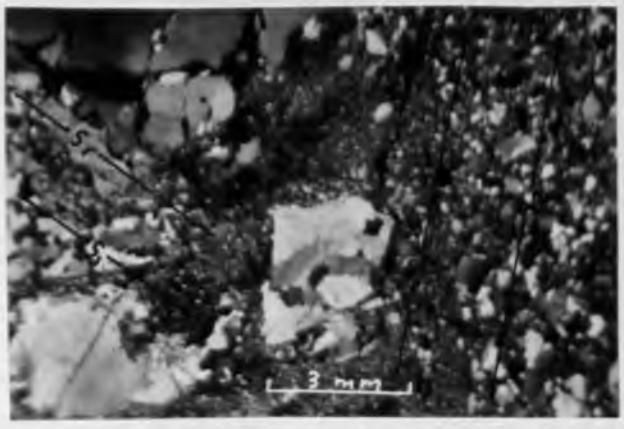

Figure 28. Photomicrograph of the contact between the banded augen gneiss and the overlying Pioneer Formation. The s_1 and s_2-surfaces demonstrate the angular unconformity between the Pioneer and the older bedrock (Pinal Schist ?). Crossed Nicols.

Figure 29. The s_2-surfaces in the granitic gneiss outlined by the parallelism of the mica flakes in the photomicrograph. Crossed Nicols.

the mountains. The relationships between the s_2- and s_3-surfaces are illustrated in Figure 32. Weakly developed s_3-planes are present in the banded augen gneiss exposures one-quarter mile east of Maverick Peak. The axial plane foliation strikes west-northwest and dips steeply to the northeast of southwest dependent upon its location on the minor folds.

S_4-surfaces

The quartz latite porphyry exposures throughout the area of study have a foliation which trends parallel to the intruded rocks. However, the foliation in the quartz latite dips in the opposite direction (Plate II). This structure has been designated as the s_4-surface and is believed to be mimetic after an original igneous platy flow structure.

S_5-surfaces

The s_5-surface is represented by the cataclastic deformation which occurred parallel to the s_2-surface. Such foliation is best developed in the granitic gneisses found in the southwestern part of the mapped area (Fig. 30). The cataclastic foliation shows all gradations from slight to very strong development, hence the spacing between the s_5-planes is quite variable. S_5-surfaces are developed in the banded augen gneiss, the granitic gneiss, and also within some of the aplitic and pegmatitic bodies.

Figure 30. Photomicrograph of a granitic gneiss which shows the s_2-surfaces outlined by the parallelism of the micas and the s_5-planes represented by the surfaces of granulation. Nicols crossed.

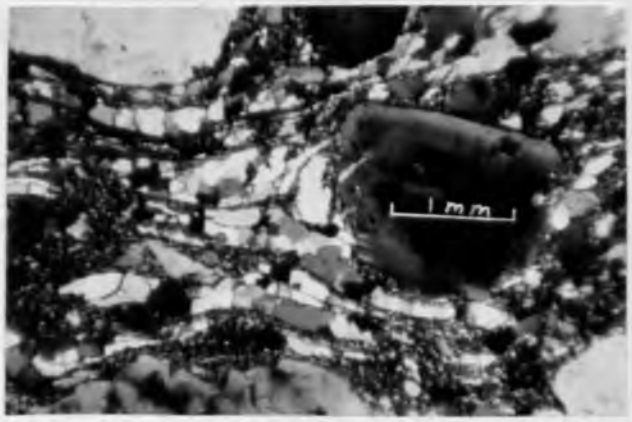

Figure 31. Recrystallized quartz in the matrix of a mylonite zone which is shown in the schematic diagram in figure 32. Nicols crossed.

S_6-surfaces

The youngest foliate structures observed are the cataclastic structures which cut across the older features. Figure 32 is a schematic diagram which illustrates the relationships seen in a road cut south of Barnum Rock. The s_6-surfaces strike N60E to N70E and dip 30 to 40 degrees to the north. These surfaces are parallel to direction of active shear joints which will be described later. The cataclastic deformation was intense and resulted in the development of mylonitic rocks (Fig. 31). The relationships between the s_2-, s_5-, and s_6-planes are shown in Figure 33.

Lineation

Parallelism of linear elements is found in most of the rocks exposed in that portion of the eastern flank of the Santa Catalina Mountains included in the present study. Three distinct types of lineation are found. Two directions were observed, one trends northeast and the other west-northwest to east-west (Plate II). The discussion of lineation will be arranged chronologically from oldest to youngest.

"b" Lineation

Both the metamorphosed Apache Group and the Catalina Gneiss near the summit of the Catalina Mountains display "b" lineation according to the terminology of Sander (1930). The

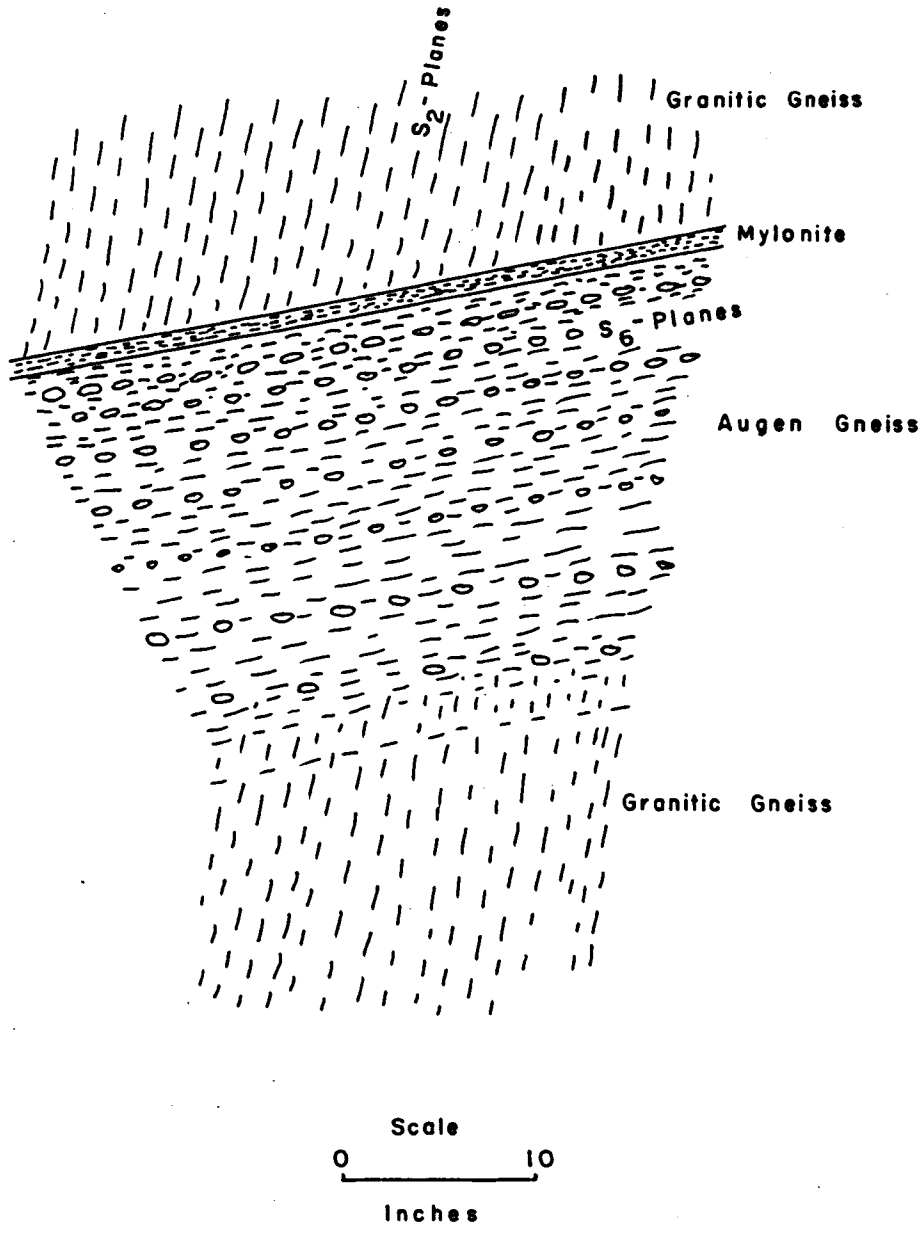

Figure 32. Schematic diagram which illustrates the s_2 and s_6 surfaces exposed in the roadcut south of Barnum Rock along the Mount Lemmon Highway. A vertical surface oriented east-west.

linear elements include parallelism of folds, dimensional orientation of crystals and pebbles, and intersections of s-planes (Fig. 35).

The characteristics of the minor folds and drag folds have been discussed previously. The micro-folds developed in the s_2-surfaces form the most obvious "b" lineation in the schistose rocks of the Pioneer Formation and Dripping Spring Quartzite. Such linear elements consist of parallel grooves or microcorrugations in the plane of foliation (s_2). The lineation trends west-northwest and plunges westward at angles of 0 to 20 degrees.

The second type of "b" lineation results from the intersection of two s-planes (Fig. 25). The s-surfaces involved are s_2 and s_3 which are bedding and axial plane foliation respectively. The trend and plunge of this lineation is the same as that described above.

The most obvious megascopic "b" lineation which results from dimensional orientation is found in the stretched pebbles and cobbles in the basal conglomerates of the Pioneer Formation and the Dripping Spring Quartzite of the Apache Group. The most pronounced elongation occurs in the Scanlan conglomerate exposed on the south slope of Kellogg Mountain. The pebbles and cobbles form cigar-shaped rods which strike N65W and plunge 15 degrees to the west-northwest. However, all of the conglomerate outcrops show elongation of the pebbles parallel to the axis of the main dome or to the minor folds. Less obvious but nevertheless

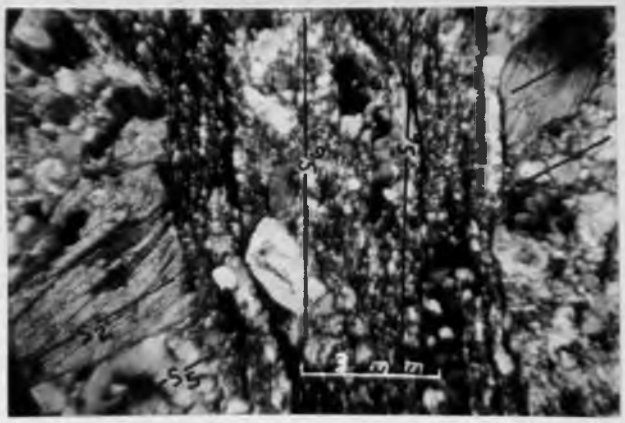

Figure 33. Photomicrograph of the Catalina Gneiss which displays s_2-, s_5-, and s_6-planes. Nicols crossed.

Figure 34. Lineation of "a" associated with the s_5-planes in Catalina Gneiss at Hitchcock Memorial. The lineation trends N45E and plunges 5° NE. Photograph taken looking northwest.

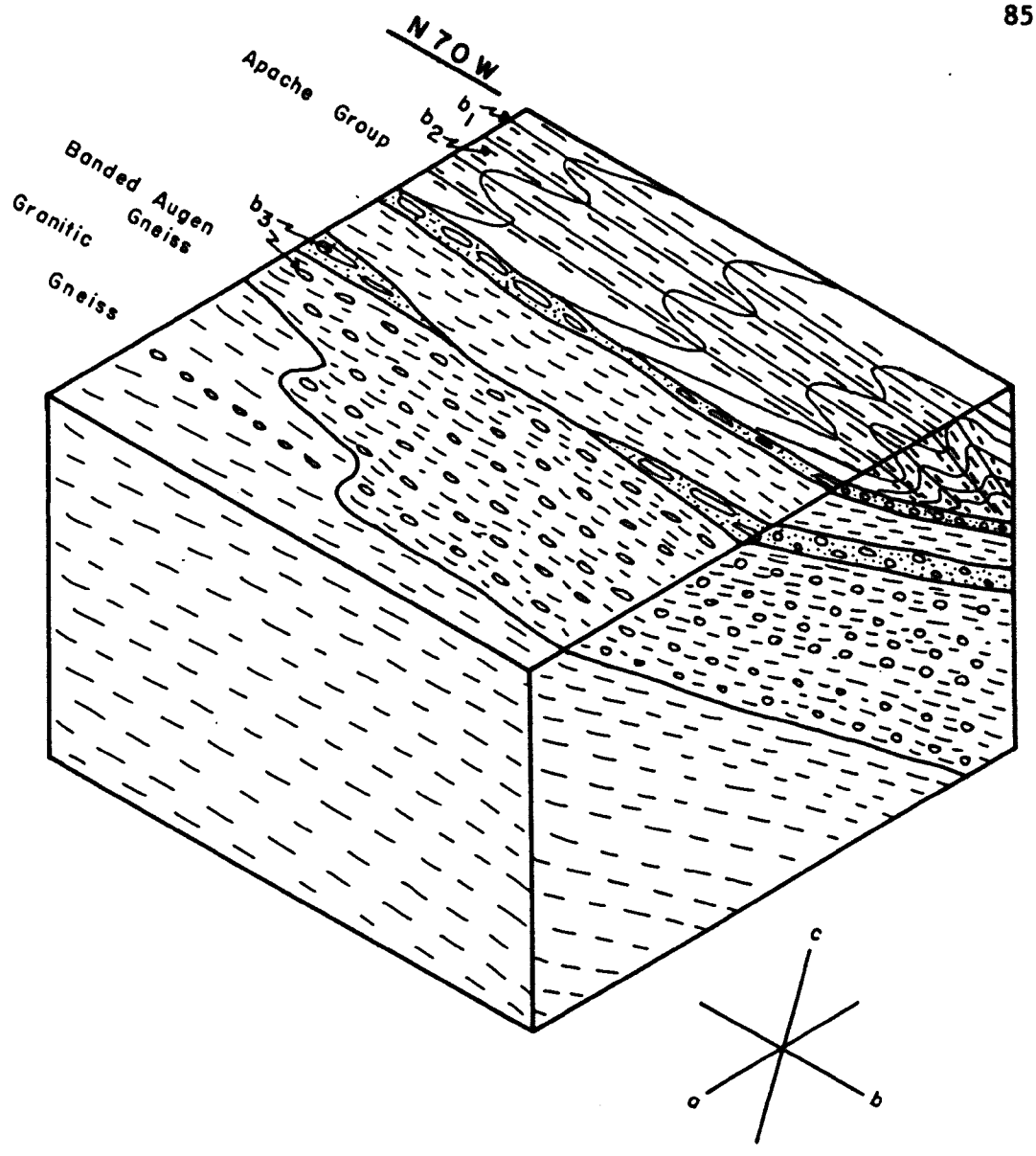

Figure 35. Block diagram which illustrates the various "b" lineations found in the rocks on the eastern side of the Catalina Mountains.

distinct is the elongation of quartz and feldspar grains in the banded augen gneiss and the granitic gneiss. The trend of the lineation varies from N70W to S80W and plunges from 0 to 20 degrees westward.

Microscopically the dimensional orientation of grains is readily apparent, for example, the elongation of quartz grains shown in Figure 25. Not only do the grains exhibit a strong dimensional orientation but also a strong optical orientation when observed under crossed nicols with the gypsum plate inserted into the microscope. The optical orientation determined in oriented thin sections reflects a "b" lineation parallel with the axes of the micro-folds Similarly studies of oriented thin sections taken from the granitic gneiss illustrates the presence of a "b" lineation which trends west-northwest just as those above.

Relict Lineation (?)

The quartz latite porphyry displays linear parallelism of feldspar phenocrysts and biotite flakes. The lineation has a remarkably uniform orientation throughout the area, varying five to ten degrees from due west. The plunge angle averages about 15 degrees to the west. The linear element in the metamorphic fabric is thought to be mimetic after flow lines in the original igneous rock.

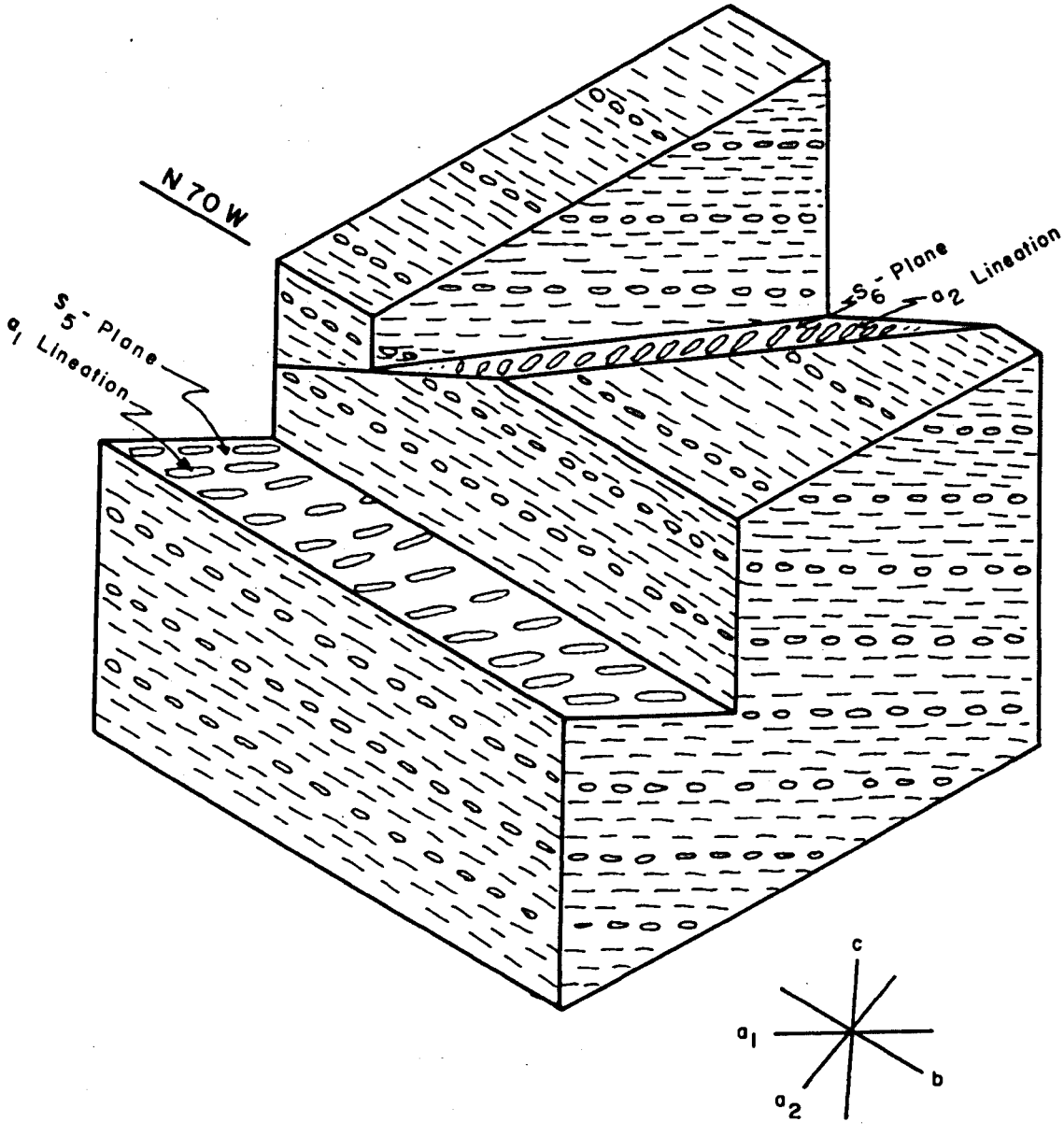

Figure 36. Idealized block diagram to illustrate the relations between the foliation and "a" lineation in the Santa Catalina Mountains.

"a" Lineation

Two distinct "a" lineations were observed in the banded augen gneiss and granitic gneiss which make up the core of the Catalina Complex (Fig. 36). The strongest developed linear element in the gneissic rocks is the elongation of quartz and feldspar grains and the streaking of micas associated with the s_5 foliation surfaces (Fig. 34). The "a" lineation trends N20E to N45E and plunges to the northeast at 5 to 20 degrees.

The second "a" lineation is found on the s_6 foliation surface. This lineation ranges from actual slickensides to the elongation of feldspar and quartz grains and the streaking out of micas by closely spaced shear planes. In the northwestern part of the area the s_6-planes strike N60E and dip to the north-northwest. The lineation on such surfaces trends N30W and plunges northward parallel to the dip of the s_6-surface. The slickensides indicate that the hanging wall moved downward relative to the footwall. In the south-central portion of the area the s_6-planes strike N80W and dip to the north-northeast. The lineation trends parallel to the direction of the dip.

Joints

The joint distribution is shown on Plate III. The major joint directions found in the northwestern part of the area trend N70W, N30W, N60E, and N20E (Fig. 37). The axis of the main dome strikes N70W in this area: hence, the joints parallel to it could

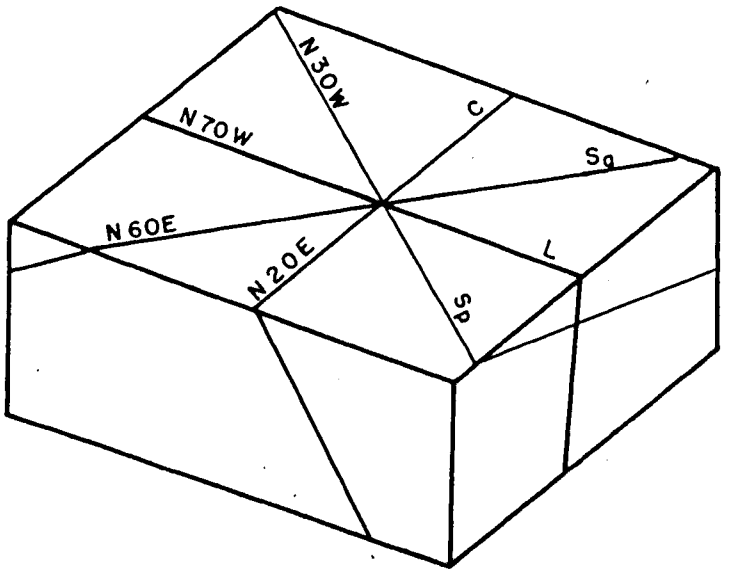

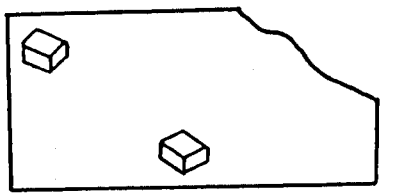

Location of blocks within map area.

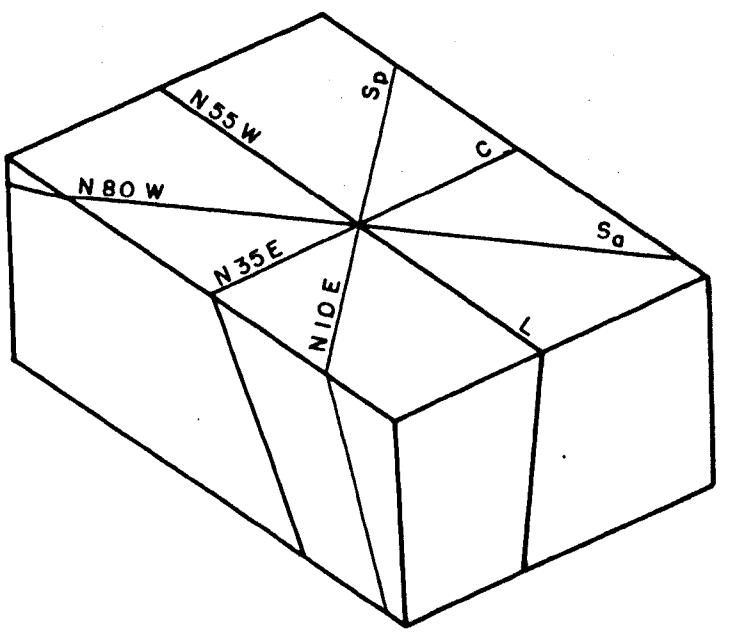

Figure 37. Idealized exploded block diagram to illustrate the changes of joint direction within the area of study. L=longitudinal joints, C=cross joints, Sa=active shear direction, and Sp= possible shear direction.

be designated as longitudinal joints, the N20E trend then would be cross joints and the remaining directions would form a conjugate shear system. The active shear direction as evidenced by the s_6-surfaces strikes N60E and dips 30 to 40 degrees to the north-northwest. In the south-central part of the area the "b" direction swings around to N55W with a complimentary change in the joint directions as follows: N55W, N35E, N80W and N10E. The first two directions correspond to the longitudinal and cross joints respectively and the last two form the shear system. The active shear direction strikes N80W and dips to the north-northeast. The longitudinal and cross joints are commonly filled with quartz. The quartz filled fractures are very commonly offset. At one place the longitudinal joints will be offset by the cross joints while at another the reverse will be true.

PETROGENESIS

Within the limits of the area of this investigation the exposed rocks are the result of a post-Paleozoic metamorphism, and only a limited number of inferences can be drawn regarding the earlier history. However, as previously mentioned, in the northern part of the Santa Catalina Mountains Older Precambrian rocks crop out extensively and their history has been described in some detail by Wallace (1954) and Banerjee (1957). Likewise the Younger Precambrian history of the Apache Group has been well summarized by Lance (1959), and Shride (1961) gives an exhaustive treatment that need not be repeated here. Inasmuch as only limited exposures of Paleozoic rocks are found in the area of the present study the reader is referred to the work of Peirce (1958) for a more complete Paleozoic history.

Younger Precambrian

After uplift and a long period of erosion the region was again downwarped and subjected to sedimentation. The general nature of the Younger Precambrian sediments and their limited thickness suggests a marginal shelf-type sedimentation. The presence of diabase sills and basaltic flows in the upper part of the section indicate mild deformation prior to Middle Cambrian times (Shride, 1961). The exact nature of the disturbance and the resultant trends are difficult to determine; however, Shride (1961) has shown that in adjacent areas the trends are north or northwest.

Paleozoic

In Middle Cambrian time the region was once again submerged and shallow water marine deposits formed. Deposition continued intermittently through the Permian. Local times of non-deposition or erosion were the only evidence of tectonic unrest. The end of the Paleozoic was marked by general uplift of the region.

Mesozoic

Triassic and Jurassic sediments have not been reported in southern Arizona (McKee, 1951). Near Peppersauce Canyon in the northern Santa Catalina Mountains a conglomerate has been tentatively dated as Lower Cretaceous (McKee, 1951). In Cienega Wash, north of the Empire Mountains and south of the Rincon Mountains, D. W. Shafroth (personal communication) has measured approximately 15,000 feet of Lower Cretaceous rocks. The Lower Cretaceous rocks consist of conglomerates at the base and top of the section. The lower conglomerates rest unconformably upon Paelozoic rocks and the upper conglomerates are unconformably overlain by rocks of Upper Cretaceous age. The Upper Cretaceous rock contains abundant volcanic debris which may be a reflection of the affects of the Laramide Orogeny.

The available field relationships in the Catalina Mountains indicate that the metamorphism is post-Paleozoic and pre-Upper Miocene. Bromfield (1952) stated that the Leatherwood Quartz Diorite intruded rocks of Cretaceous age; however, the

present author has not observed intrusive relationships between the Leatherwood and rocks younger than Upper Paleozoic. Furthermore, the rocks which were shown as Cretaceous on the geologic map published by Bromfield (1952) were interpreted to be Paleozoic by Raabe (1959) on the basis of their lithology. Post-metamorphism andesite dikes found within the area of study are texturally and petrographically similar to the turkey-track porphyry which Cooper (1961) reports to be Miocene in age. The Pantano sediments along the south flank of the mountains contain fragments of the Catalina Gneiss indicating that by Upper Miocene erosion had reached the core of the Catalina complex. Geochemical dating of the Catalina Gneiss at Hitchcock Monument gives an age of approximately 100 million years according to Dr. P. E. Damon (personal communication).

The metamorphism which was responsible for the characteristics of the rocks now exposed within the area under study apparently began at a considerable depth. The minimum cover which was present includes approximately 20,000 feet of Younger Precambrian, Paleozoic, and Lower Cretaceous rocks. The linear distribution of metamorphism parallel to the axis of doming suggests that the two might be related. The metamorphism is a regional type which has a limited areal extent and which increases in intensity as the gneissic core is approached.

The mineral assemblages developed in the rocks exposed throughout most of the area mapped are indicative of medium- to high-grade zones of progressive regional metamorphism of the

Barrovian type. Four chemical classes of rocks are found which include pelitic, quartzo-feldspathic, calcareous, and basic igneous rocks. The chemical compositions of the pelitic rocks and the quartzo-feldspathic rocks will be portrayed on AKF diagrams. The AKF diagrams are prepared as follows: A is equal to Al_2O_3 minus (CaO plus Na_2O plus K_2O), K equal K_2O, and F equal FeO plus MgO plus MnO. Such diagrams are based upon the assumption that the various oxides which are grouped together will act as one chemical component, and have been used by Turner (1948) and Turner and Verhoogen (1960) to express the chemical and mineralogical compositions of metamorphic rocks. Several workers in the field, for example, Ramberg (1952) and Thompson (1957) have suggested the use of tetrahedral diagrams which give a more accurate representation. The facies classification given by Turner and Verhoogen (1960) will be followed and for that reason the chemical compositions have been presented on AKF diagrams. The chemical compositions determined from the modal analyses were used to prepare the diagrams. Figure 38 represents the plot of all the modal analyses which will fall on an AKF diagram. The diagrams in Figures 39 through 42 illustrate the plots for individual rock units and show changes in bulk composition between rock units.

The pelitic rocks are characterized by a mineral assemblage of quartz-muscovite-biotite-microcline-oligoclase (An_{20-25})-epidote which would place them into the staurolite almandine subfacies of the almandine amphibolite facies of Turner and Verhoogen.

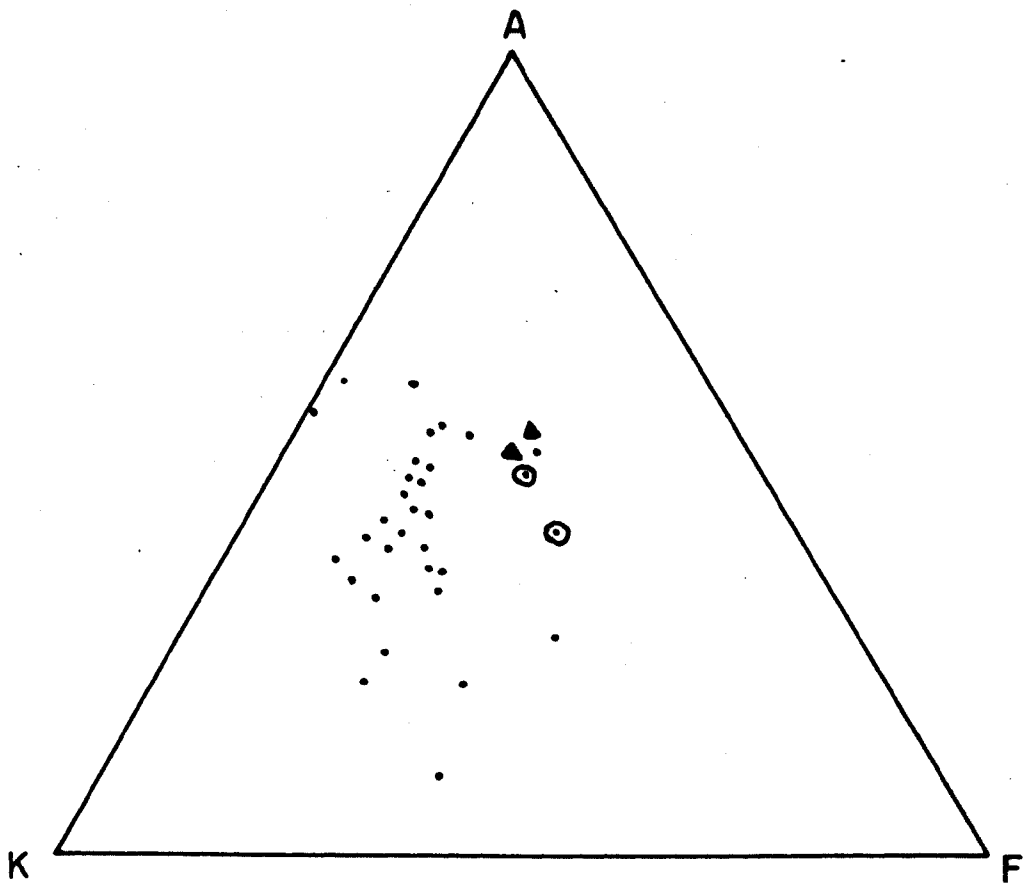

Figure 38. AKF diagram based upon the oxide percentages determined from modal analyses for representative rocks in the map area. The triangles represent inclusions in the banded augen gneiss. The circled dot represent Pinal schist based upon chemical analyses made at the Rock Analysis Laboratory, University of Minnesota, for A. K. Banerjee under a Geological Society of America grant.

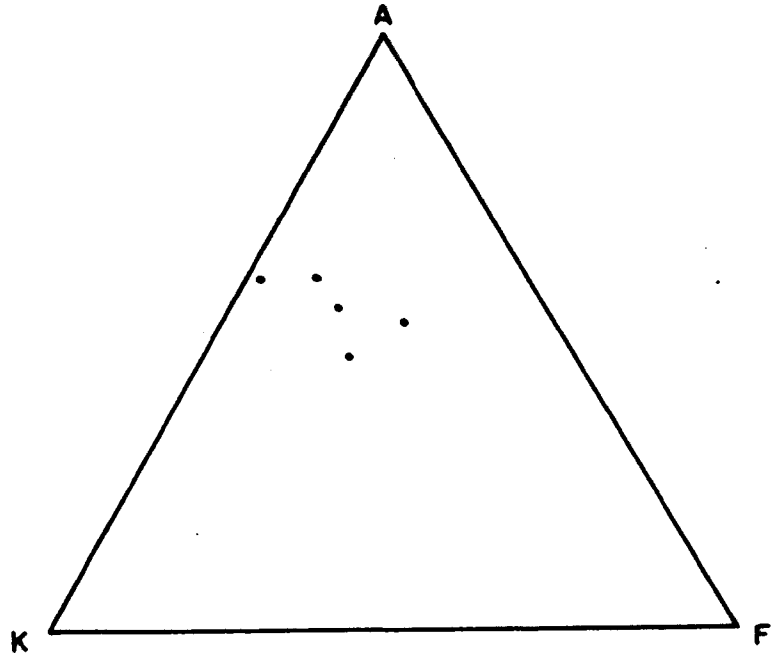

Figure 39. AKF diagram for rocks of the Pioneer member of the Apache group. Based upon modal analyses.

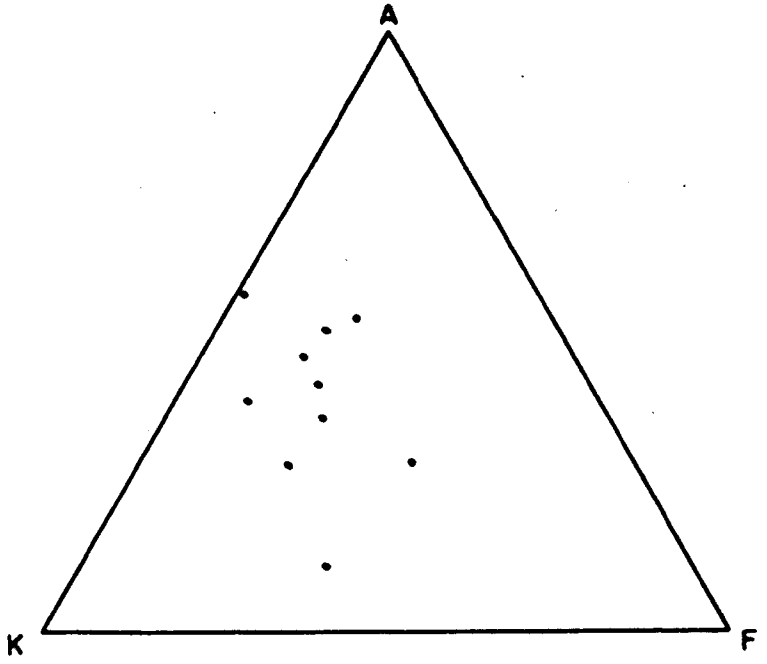

Figure 40. AKF diagram for the Dripping Spring quartzite member of the Apache group. Diagram based on results of modal analyses.

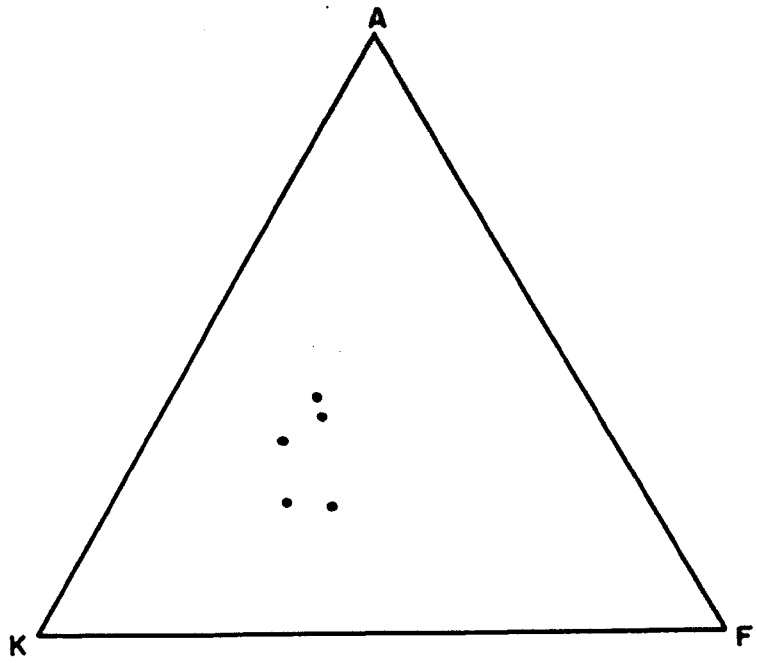

Figure 41. AKF diagram of the banded augen gneiss based upon results of modal analyses.

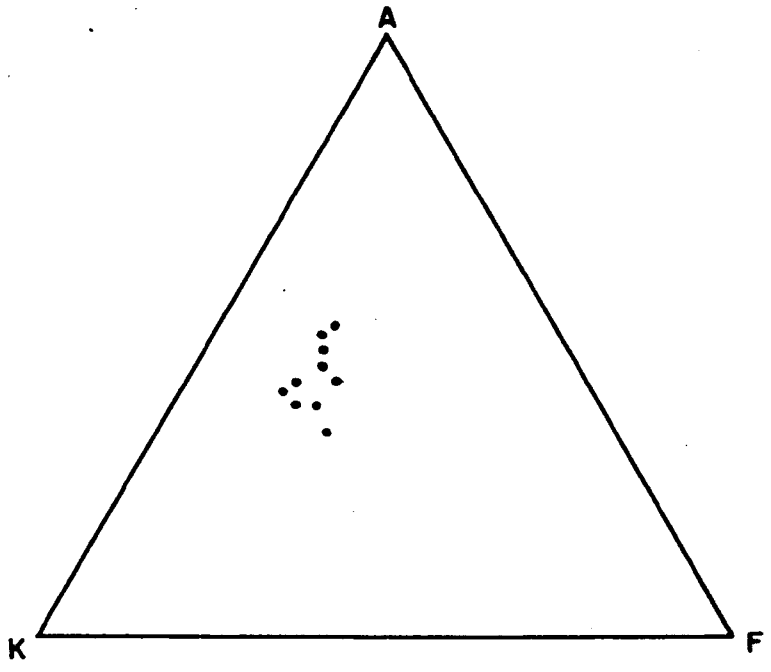

Figure 42. AKF diagram based upon the results of modal analyses of the granitic gneisses exposed in the core of the Santa Catalina Mountains.

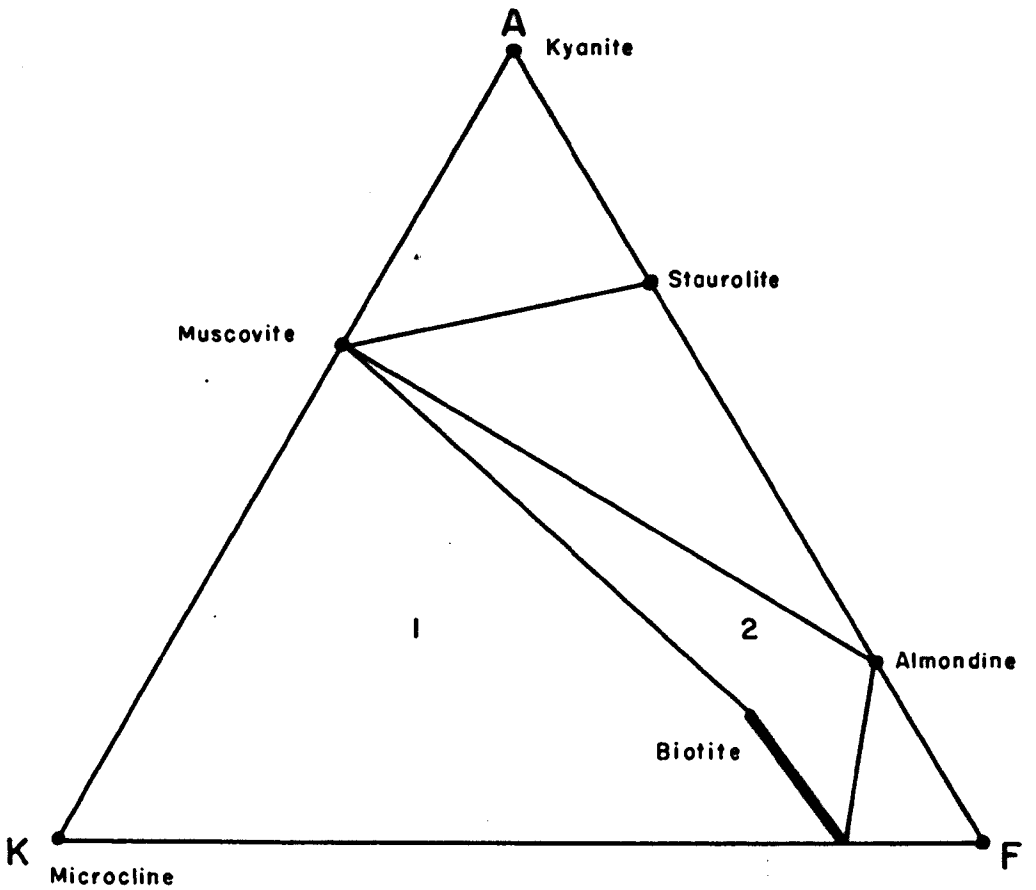

Figure 43. Almandine Amphibolite Facies, Staurolite-almandine Subfacies. AKF diagram for rocks with excess SiO_2 and Al_2O_3. Quartz, plagioclase, and epidote are possible additional minerals. After Turner and Verhoogen, 1960.

Figure 43 is the AKF diagram for rocks with an excess of SiO_2 and Al_2O_3 and the above mineral assemblage falls into the field designated (1). The garnet-bearing Dripping Spring Quartzite is typified by the minerals of field (2) and contain quartz and microcline as well. With the exception of a minor amount of hornblende-bearing schist in the upper Dripping Spring and the quartzo-feldspathic units of the Dripping Spring Quartzite the remainder of the Dripping Spring and Pioneer Formation have the pelitic assemblages given above.

The quartzo-feldspathic rocks include part of the Dripping Spring Quartzite, the banded augen gneisses, and the granitic gneisses. Quartzo-feldspathic members of the Dripping Spring Quartzite are characterized by quartz-microcline-oligoclase (An_{20-25})-muscovite-biotite (-epidote may be an additional phase) which place them into field (1) of Figure 43. The banded augen gneisses are also characterized by the above mineral assemblage. The granitic gneisses are typified by the association of quartz-microcline-oligoclase (An_{20-25})-muscovite-biotite-almandine. The four phase assemblage given above suggests that we are not dealing with an equilibrium assemblage. Furthermore, the gneissic rocks contain an intermediate potash feldspar, as previously discussed, which does not conform to the equilibrium assemblage as shown in Figure 43.

In order to attempt an explanation of the discrepencies found in the optics of the potash feldspars several samples were examined by means of X-ray diffraction techniques with a diffrac-

tometer. According to Harker (1954) the presence of microcline and orthoclase can be determined by the d_{130} and $d_{1\bar{3}0}$ spacings (Fig. 44a). The results of the method applied to the larger crystals, optically identified as microcline, in the Catalina Gneiss confirm the microcline identification as shown in Figure 44b. However, X-ray examination of the interstitial potassium feldspar from the granitic gneiss and banded augen gneiss as well as larger crystals from pegmatitic veins yield a pattern similar to that given by Harker (Fig. 44c) which suggests that both phases are present within individual grains. The textural relationships indicate that the orthoclase is developing from microcline and suggests that the mineral assemblage might not be indicative of the staurolite almandine subfacies as defined by Turner and Verhoogen (1960). Francis (1956) states that orthoclase may appear in rocks which he defined as the kyanite-muscovite-quartz subfacies. The AKF diagram proposed by Francis is identical with Figure 43 except that orthoclase appears along with microcline at the K apex. Therefore, the rocks containing orthoclase as well as microcline are tentatively assigned to the kyanite-muscovite-almandine subfacies of the almandine amphibolite facies (Turner and Verhoogen, 1960). Furthermore, the mineral assemblage is believed to be a non-equilibrium assemblage transitional between the two facies.

A second discrepancy which must be accounted for is the general lack of almandine in the pelitic rocks, and the conspicuous garnet development within the granitic gneiss, aplites,

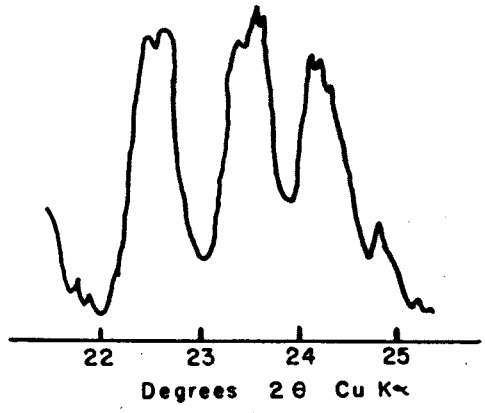

(a)

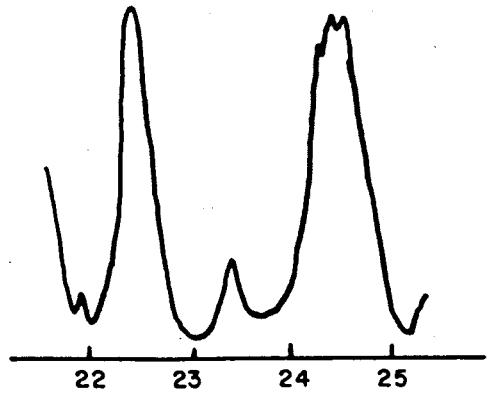

(b)

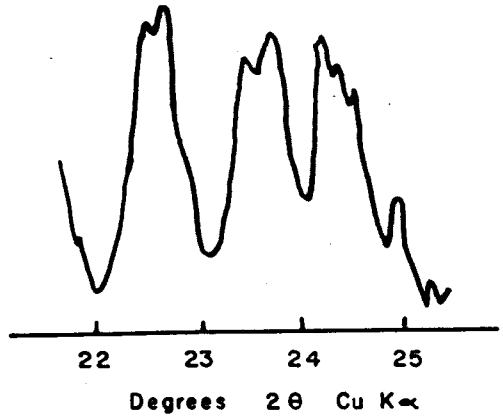

(c)

Figure 44. (a) represents the curves given by Harker (1956) for the feldspars in a granitic gneiss in which orthoclase is being converted to microcline by metamorphism. The inner peak is the d_{130} of orthoclase while the outer two represent the d_{130} and $d_{1\bar{3}0}$ for microcline. (b) Microcline pattern for large crystals in granitic gneiss. (c) Microcline being converted into orthoclase.

and pegmatites. The lack of garnet formation in the pelitic rocks can be related to the high potash content as shown by comparison of Figure 38 and 43. Only a few of the analyzed rocks have a composition which falls within the muscovite-biotite-almandine field. Similarly, the composition of the garnetiferous granitic gneiss plots outside of the above field, that is the gneissic rocks are as rich in potassium as the pelitic rocks, so that some other explanation must be called upon. The textural features found in the majority of granitic gneisses in the mapped area suggests that they may have originally been igneous rocks. Therefore, the modal plagioclase, potash feldspar, and quartz determined from thin section study were plotted on a ternary diagram (Fig. 45). Then the results from each of the rock units were plotted separately as shown in Figures 46 to 49. Chayes (1951) prepared a diagram for modal plagioclase, orthoclase, and quartz for 260 thin sections of granites in the eastern United States. He found that the modal composition coincided with the thermal valley of Bowen (1937). Chayes concluded that the distribution of analyses favored a magmatic origin for such rocks. Similarly the analyses of Chayes coincide with the minimum point on the diagram for the system SiO_2-$NaAlSi_3O_8$-$KAlSi_3O_8$ given by Tuttle and Bowen (1958), which they also interpret as strong evidence for a magmatic origin of the rocks. In Figures 48 and 49 the zero, two, and five per cent contours of Chayes diagrams have been superposed upon the analyses of the gneissic rocks of the Santa Catalina Mountains. The modal composition of the granitic gneiss falls

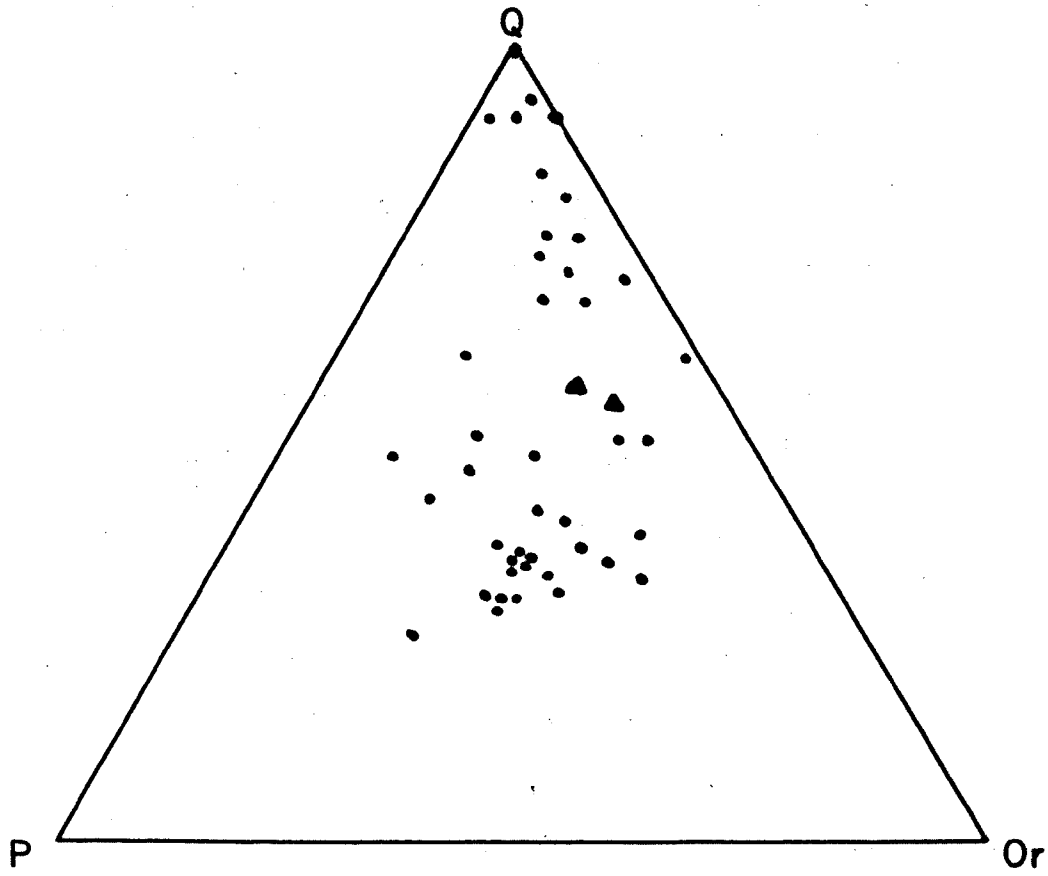

Figure 45. Modal plagioclase, potash feldspar, and quartz from various rocks in the Catalina Mountains.

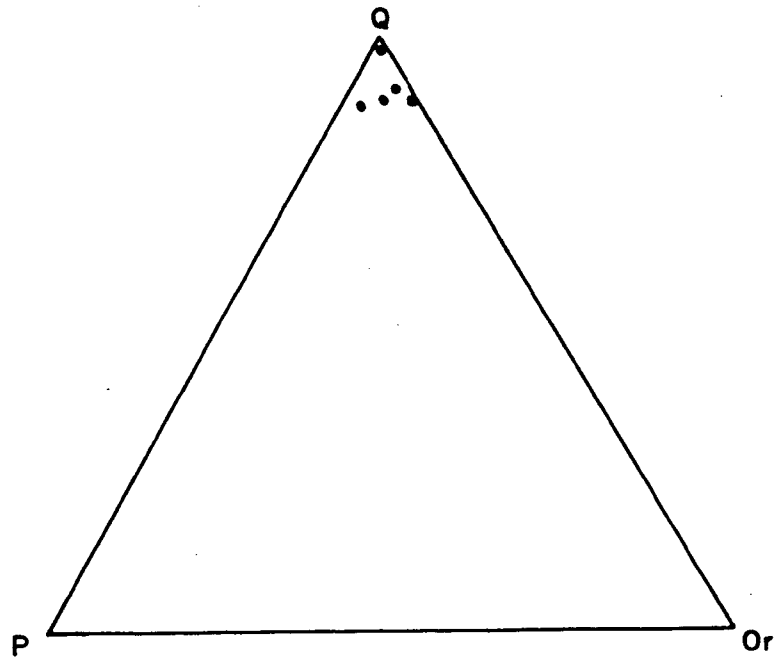

Figure 46. Modal plagioclase, potassium fledspar, and quartz found in the Pioneer Formation of the Apache group.

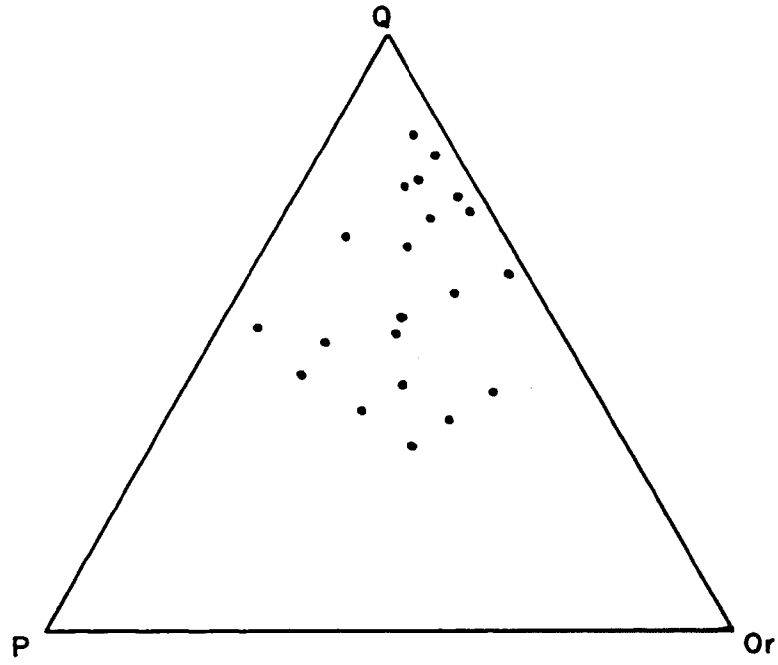

Figure 47. Modal plagioclase, potash feldspar, and quartz from twenty thin sections of the Dripping Spring Quartzite.

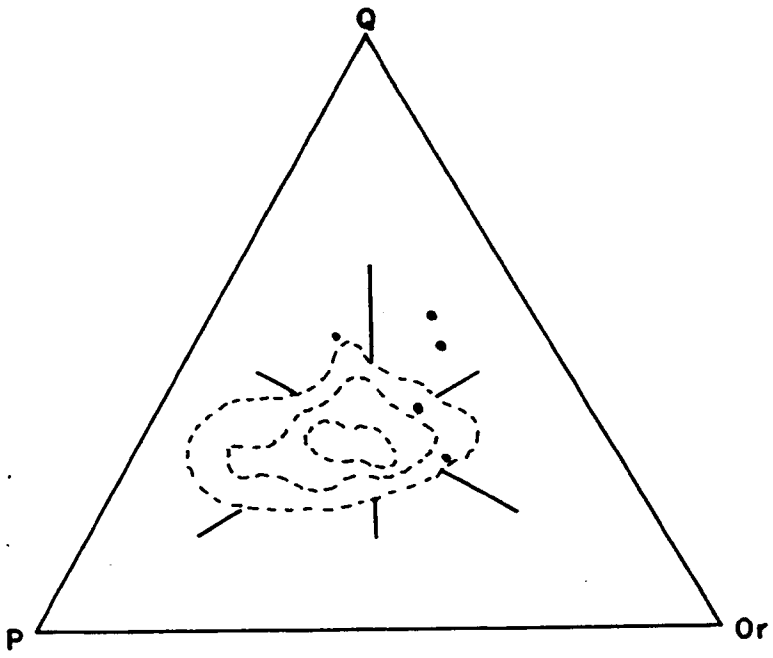

Figure 48. Modal plagioclase, potash feldspar, and quartz in the banded augen gneiss. The zero, two and five per cent contours of Chayes are also shown.

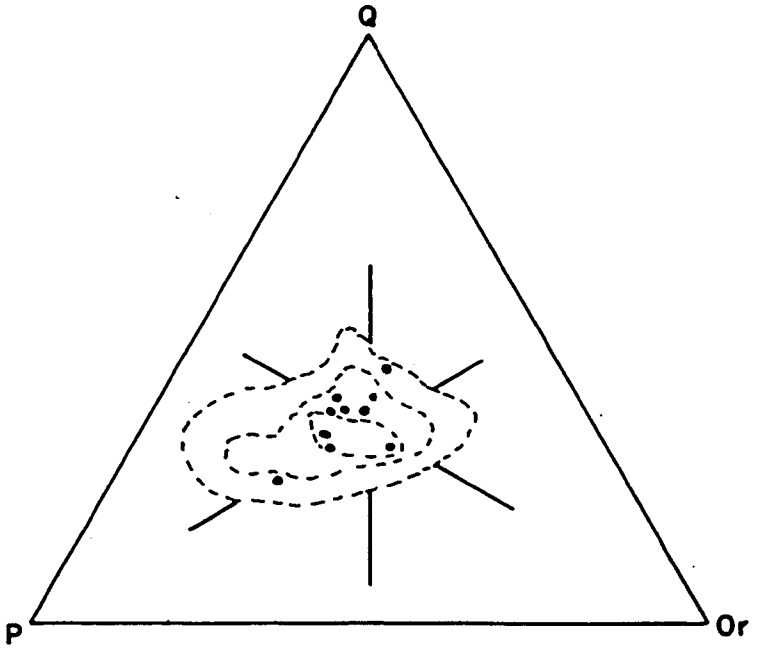

Figure 49. Modal plagioclase, potassium feldspar, and quartz in ten thin sections of granitic gneiss. The zero, two, and five per cent contours of Chayes are superposed.

close to the maxima whereas the banded augen gneiss and the Apache metasediments fall outside and toward the quartz apex. Thus the combination of textures and modal compositions suggests that the granitic gneisses were derived from igneous rocks. Regional metamorphism of granitic igneous rocks commonly results in the formation of garnet. Ramberg (1952) considers the formation of garnets by the following reactions: (1) biotite+muscovite+ quartz $\rightleftharpoons$ orthoclase + almandine + water and (2) Fe,Mg-chlorite +quartz $\rightleftharpoons$ Fe,Mg-garnet+ water. If the original igneous rock had a granodioritic composition the metamorphism would develop epidote, muscovite, and a more sodic plagioclase from the original plagioclase. Then the newly formed muscovite could react with original biotite according to equation (1) and any chlorite in the original igneous rock would react according to equation (2) to produce garnet. The composition of the garnets found in the granitic gneiss (Pilkington, 1961) and the small quantity of epidote found in the gneisses suggests that much of the calcium released by the breakdown of the original plagioclase enters into the formation of the garnets. Also effects of Mn upon the above reaction would have to be taken into consideration since its presence is indicated by the spessartite content of the resultant garnets.

The mineral assemblages found in the metamorphosed Mescal Limestone, diabase, and Abrigo Limestone would also place them in the staurolite almandine subfacies (Turner and Verhoogen, 1960). However, the chemical composition can better be considered

in terms of the ACF diagram (Fig. 50) given by Turner and Verhoogen (1960). After correction for the accessory minerals (Turner and Verhoogen, p. 504) A, C, and F are calculated so that $A = Al_2O_3 + Fe_2O_3 - (Na_2O + K_2O)$; $C = CaO$; $F = MgO + FeO + MnO$. The metamorphosed diabase consists of hornblende-oligoclase (An_{20-25})-biotite-epidote-quartz mineral assemblages. The Mescal Limestone has been converted into one of the following: calcite-tremolite-epidote-diopside or into calcite-tremolite-chlorite rocks. The Chlorite minerals, as previously discussed, consist of penninite and prochlorite both of which are magnesium-rich minerals. The presence of such chlorites is compatible with the other minerals in the amphibolite facies according to Yoder's (1952) experiments and also according to Fyfe, Turner, and Verhoogen (1958). The diversified nature of the Abrigo lithology gives rise to mineral assemblages which may be shown on either Figure 43 or 50. The argillaceous portions of the formation are characterized by quartz-muscovite-biotite-microcline-oligoclase of field (1) Figure 43. The high potash content in the area of the present study prevented the formation of staurolite; however, Peirce (1958) reports staurolite from the lower argillaceous units within the Abrigo Limestone in the vicinity of Summerhaven. The more calcareous layers of the Abrigo are typified by plagioclase (An_{25-40})-hornblende-diopside-epidote-microcline-quartz; or by plagioclase (An_{25-65})-grossularite-diopside-epidote-microcline-quartz; or by diopside-calcite-microcline-quartz. The epidote minerals in the above assemblages

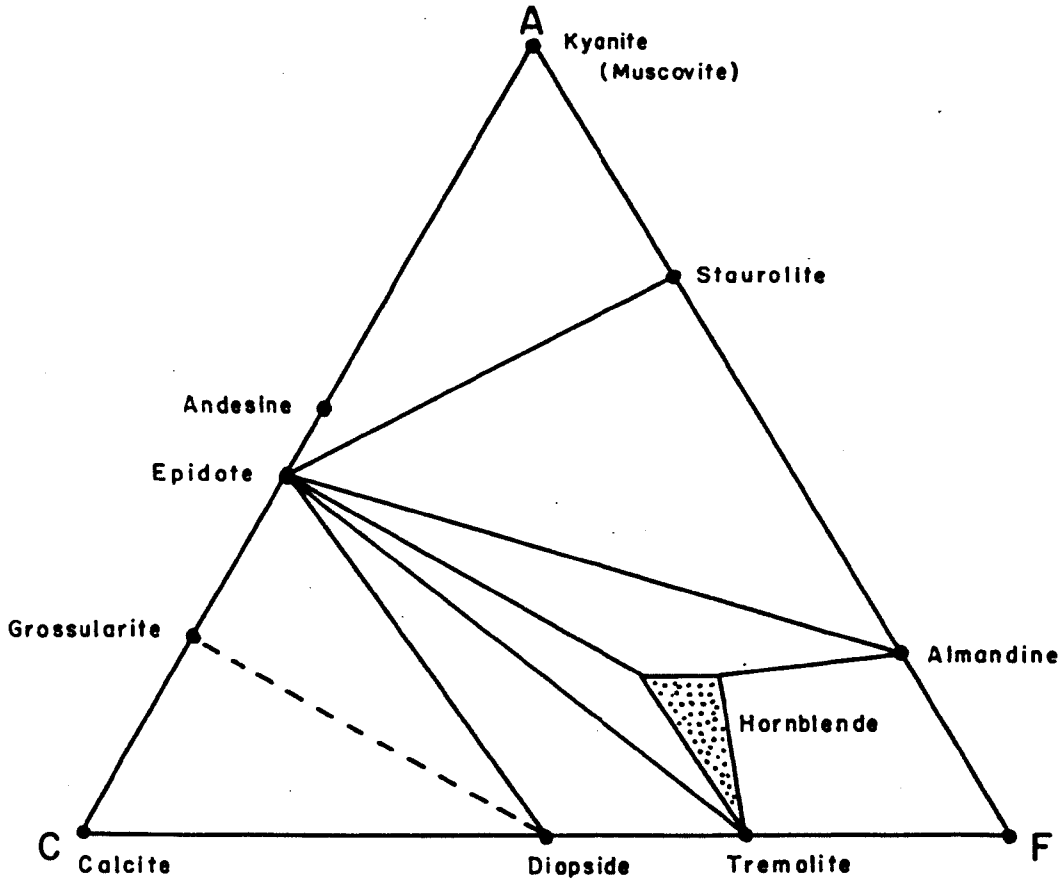

Figure 50. Almandine Amphibolite Facies, Staurolite-almandine Subfacies. ACF diagram for rocks with an excess of Al_2O_3. Quartz and plagioclase (An_{20-50}) are additional phases. Microcline occurs only in rocks lacking kyanite, staurolite, or almandine. After Turner and Verhoogen (1960).

include clinoziosite, zoisite, and normal epidote. The term hornblende has been used for common green hornblende, tremolite, and tschermakite. Similarly the diopside may refer to either diopside or hedenbergite. The compositional variation in the anorthite content of the plagioclase appears to be directly related to the K_2O content of the rocks. In the staurolite almandine subfacies the stable potash feldspar is microcline, and it will form whenever the ratio of $(CaO+K_2O+Na_2O)$ to Al_2O_3 exceeds unity. The formation of microcline used part of the Al_2O_3 and Na_2O, but since there was an excess of alumina, plagioclase (An_{25-65}) formed until all the Na_2O was used up, then epidote formed to utilize the remainder of the Al_2O_3. Thus the apparent contradiction of epidote and calcic plagioclase co-existing in the same rock is related to the high potash content. Original dolomitic layers in the Abrigo Limestone are represented by the assemblage of tschermakite-tremolite-vesuvianite. The presence of vesuvianite indicates a high partial pressure of water.

The textural relations shown in the metamorphic rocks indicate that crystallization and recrystallization reached a maximum during the period of deformation, and that the deformation outlasted crystallization. Therefore, it would be desirable to explain both the metamorphism and the deformation by the same mechanism. It is proposed that the formation of a mantled gneiss dome could explain the observed features.

The mechanism of formation of the mantled gneiss dome is believed to be similar to that proposed by Eskola (1948) in which the doming is related to the remobilization of the basement complex. In the Santa Catalina Mountains the basement complex included granitic rocks, such as the Oracle Granite, and the enclosing metamorphic rocks of the Pinal Schist (Banerjee, 1957). Within the area of study no rocks resembling the Pinal Schist were found. However, the unconformable relationship between the s_1- and s_2-surfaces at the contact between the banded augen gneiss and the Pioneer Formation suggest that the banded augen gneiss might be equivalent, at least in part, to the Pinal Schist. In addition the banded augen gneiss contains numerous inclusions of incompletely feldspathized metasediments which are similar to the Pinal schist as shown in Figure 38. Finally, the original sedimentary nature of the banded augen gneiss is suggested by the distribution of modal quartz, plagioclase, and potash feldspar as shown on Figure 48. The granitic gneiss within the area investigated represent the granitic rocks of the original basement complex. Upon this basement complex a probable minimum of 20,000 feet of Younger Precambrian, Paleozoic, and Lower Cretaceous rocks were deposited.

The second stage in the development of the mantled gneiss dome, therefore, began at a considerable depth. If a geothermal gradient of $30^{\circ}C/km$ is assumed the temperature at the contact between the basement complex and the overlying sedimentary pile would have been a minimum of approximately $200^{\circ}C$. The temperature

at a depth of 10 km would have been 300°C. Hedge (1960) used the sodium-potassium ratios in muscovites as a geothermometer and reports temperatures of 460°-620°C for the rocks within the area of the present study. The maximum temperature which Hedge reported was for the Catalina Gneiss near the contact with the Apache Group which based upon the above geothermal gradient indicate a depth of burial of 20 kilometers. An alternative explanation could be that the temperatures were developed at the minimum depth previously postulated as a result of a much higher geothermal gradient. It would appear reasonable to assume that the actual situation in the Catalina Mountains represents conditions between the two extremes. The elongated nature of the dome and the distribution the varying degrees of metamorphic intensity are suggestive of a deep seated zone of weakness which may have acted as a channelway for the transfer of heat.

The orientation of the shear joints suggests that the formation of the dome was brought about by vertical forces. At the temperatures suggested by the geothermometry studies the basement rocks could be expected to behave as a rheid (Carey, 1953) and if a zone of weakness existed might be expected to flow upwards. An additional motivating force which should be considered is the mechanism of partial melting proposed by Tuttle and Bowen (1958). Partial melting would begin in granitic rocks at a temperature of 640°C at a pressure of 4000kg/cm^2. Based upon the calculations of Tuttle and Bowen

a granite containing 10 per cent biotite as the hydrous phase would begin to melt under the above conditions if it contained as little as 0.5 per cent water. The depth of partial melting at an assumed geothermal gradient of 30°C/km would be 21 kilometers. On the other hand if we assume a gradient which would give a temperature of 620°C at a depth of 6.7 km then partial melting would occur at a depth of approximately 8.0 kilometers. The mechanisms proposed by Tuttle and Bowen would account for (1) the motivating force for the upward movement of the dome, and (2) within the zone of partial melting provide a lubricating media to increase mobility, both physical and chemical. The upward movement of the basement complex resulted in the doming of the overlying sediments. The differences in rheidity resulted in increased stresses in the sedimentary cover which, coupled with the increased temperatures, were sufficient to initiate metamorphism. Thus the sediments were synkinematically metamorphosed in response to the doming of the basement complex.

It is suggested that the banded augen gneiss developed as a result of metasomatism associated with doming. The term metasomatism is used in the sense of Lindgren (1933) who stated it as follows: "The process of practically simultaneous capillary solution and deposition by which a new mineral of partly or wholly differing chemical composition may grow in the body of an old mineral or mineral aggregate." Thus it includes the redistribution of constituents of local derivation as well as materials which were introduced. The presence of incompletely

feldspathized inclusions within the banded augen gneiss has been mentioned. In addition the contacts between the banded augen gneiss and the Pioneer Formation along Buehman Canyon are gradational in many places. The gradational contacts are characterized by the development of feldspar porphyroblasts in the rocks of the Apache Group which decrease in number away from the contact. In several places the metasomatism has converted all the Pioneer Formation into banded augen gneiss (Plate II). The modal distribution of quartz, plagioclase, and potash feldspar in the banded augen gneiss falls between the plots for the Pioneer rocks and those of the granitic gneiss which suggests that metasomatism may have been active and resulted in the conversion of the original sediments into a more granitic appearing rock. Such a mechanism is a common feature associated with mantled gneiss domes as pointed out by Eskola (1948) and Chapman (1939). The metasomatism is postulated to be the result of redistribution of materials within the original sediments and the introduction of materials from within the zone of partial melting.

As the dome rose the bedding (s_1-planes) of the basement rocks was destroyed by the development of the s_2-surfaces related to differential movements in response to the rise of the dome. The local preservation of the s_1-planes is believed to be the result of the relief of stresses by slippage in the nearby incompetent Pioneer Formation. Drag folds developed in the incompetent layers of the Apache rocks and formed a conspicuous "b" lineation. Flexure-slip folds and associated axial plane foliation formed

in the later stages of metamorphic crystallization. The intersection of the axial plane foliation with the s_2-surfaces gives rise to a distinct "b" lineation. Dimensional orientation of individual grains and the elongation of pebbles and cobbles in the conglomeratic rocks are related to the extension of the rocks parallel to the axis of the dome as the dome height increased.

Late-kinematic intrusion of quartz latite porphyry dikes along tension cracks on the flank of the dome resulted in well-developed platy and linear flow structure. Mimetic recrystallization preserved both or the original structures. The quartz latite represents magma derived from the zone of melting in the deeper portions of the dome.

Differential movements within the granitic gneiss core became more and more cataclastic in nature as the rising dome reached thermal equilibrium with its surroundings. However, the still mobile materials at depth continued to push upward and the s_5-planes developed as a result of slippage along the older planes of foliation (s_2) in the viscous portions of the dome. The differential movement on the s_5-surfaces developed the pronounced "a" lineation in the granitic gneiss. As the mass became more rigid the differential movements were taken up by the maximum shear directions which produced the s_6-planes. Slippage along the minutely spaced shear planes resulted in the formation of the second direction of "a" lineation found in the local mylonitic rocks.

Late-kinematic to post-kinematic aplitic to pegmatitic bodies are common in the metasediments and gneissic rocks as previously mentioned. The bodies were not studied in detail, but the field and petrographic observations made suggest a replacement origin for many of the aplites and pegmatites in the gneissic rocks. While many of the masses are extremely irregular, most appear to be related to the tensional joint directions. Within the gneissic rocks the majority of aplites and pegmatites contain relict structures which are parallel to the foliation in the adjacent rocks. The contacts may be sharp or gradational. Occasionally a cross-cutting body is found which has dragged the foliation of the country rocks around until it is subparallel to the dike walls. The aplitic and pegmatitic masses which contain relict foliation are believed to have originated through metasomatism along zones of weakness which existed before the joints came into existence and continued after the rock had become sufficiently rigid to yield by rupture. The second type which deformed the foliation in the country rocks represent the intrusion of more mobile materials along zones of weakness while the country rocks were still somewhat plastic. The aplitic and pegmatitic bodies in the metasedimentary rocks appear to have been emplaced in a very mobile state and may represent a crystal mush lubricated by an interstitial melt.

SUMMARY

The detailed structural and petrological studies of the present investigation have brought out several significant facts concerning the geology of the Santa Catalina Mountains. The distribution of rock types in a heretofore little known portion of the Catalina Mountains has been mapped in detail. The establishment of an unconformity at the base of the conglomeratic or schistose rocks in Buehman Canyon substantiates the previous correlation of the medium-grade, synkinematically metamorphosed conglomerates and schistose rocks along the crest of the range with the less metamorphosed Apache Group in the northern part of the Catalina Mountains. The presence of the Mescal Limestone in the Younger Precambrian section has been established stratigraphically, and its distribution within the area of the present study mapped.

The petrography of the various rock units has been worked out in detail. The petrographic descriptions include the nature of the medium- to high-grade metamorphic rocks and interpretations as to the nature of the original materials from which the rocks were derived. The mineralogical assemblages found in the metasediments adjacent to the granitic gneiss core confirmed the placement of the rocks into the staurolite-almandine subfacies of the almandine amphibolite facies of regional metamorphism. The development of orthoclase in the gneissic rocks has been interpreted as indicating the transition into the

kyanite-muscovite-almandine subfacies in the core of the complex. The distribution of modal quartz, plagioclase, and potash feldspar in the granitic gneiss lends strong support to the conclusion that the parent materials for the gneisses were igneous rocks. Similarly, the distribution of the same materials in the banded augen gneisses combined with the textural and field relationships presents a good argument for their derivation from original sedimentary rocks.

Finally the structural mapping combined with petrographic study established the presence of six different foliation surfaces in the rocks. The relationships between the two reported directions of lineation and the various foliation surfaces have been related to the formation of a mantled gneiss dome.

BIBLIOGRAPHY

Banerjee, A. K., 1957, Structure and petrology of the Oracle Granite, Pinal County, Arizona: Ph.D. dissertation, University of Arizona.

Bowen, N. L., 1937, Recent high-temperature research on silicates and its significance in igneous petrology: Am. Jour. Sci. vol. 33, p. 1.

Bromfield, C. S., 1952, Some geologic features of the Santa Catalina Mountains: Ariz. Geol. Soc. Guidebook I, p. 51.

Carey, W. S., 1953, The rheid concept in geotectonics: Jour. Geol. Soc. Australia, vol. 50, p. 67.

Chapman, C. A., 1939, Geology of the Mascoma Quadrangle, New Hampshire: Geol. Soc. Am. Bull. vol. 50, p. 127.

Chayes, F., 1951, Modal composition of granites: Carnegie Inst. of Washington Year Book no. 50, p. 41.

Cooper, J. R., 1961, Turkey-track porphyry--A possible guide for correlation of Miocene rocks in southeastern Arizona: Ariz. Geol. Soc. Digest vol. IV, p. 17.

Damon, P. E., 1959, Geochemical dating of igneous and metamorphic rocks in Arizona: Ariz. Geol. Soc. Guidebook II, p. 16.

Darton, N. H., 1925, A resume of Arizona geology: Ariz. Bur. Mines Bull., Geol. Ser. no. 3.

Davis, W. M., 1931, The Santa Catalina Mountains, Arizona: Am. Jour. Sci., 5th Series, vol. 22, p. 289.

DuBois, R. L., 1959, Petrography and structure of a part of the gneissic complex of the Santa Catalina Mountains, Arizona: Ariz. Geol. Soc. Guidebook II, p. 117.

Erickson, R. C., 1962, Petrology and structure of an exposure of the Pinal Schist, Santa Catalina Mountains, Arizona: M.S. thesis, University of Arizona.

Eskola, P. E., 1948, The problem of mantled gneiss domes: Quar. Jour. Geol. Soc. London, vol. 104, p. 461.

Francis, G. H., 1956, Facies boundaries in pelites of the middle grades of regional metamorphism: Geol. Mag. vol. 93, p. 353.

Fyfe, W. S., Turner, F. J., and Verhoogen, J., 1958, Metamorphic reactions and metamorphic facies: Geol. Soc. Am. Memoir 73.

Harker, R. I., 1954, The occurrence of orthoclase and microcline in the granitic gneisses of the Car Chuinneag-Inchbae complex, E. Rosshire: Geol. Mag. vol. 91, p. 129.

Hedge, C. E., 1960, Sodium-potassium ratios in muscovites as a geothermometer: M.S. thesis, University of Arizona.

Jinks, J. E., 1961, The Margaret Wash section of the Mogul Fault, Pinal County, Arizona: M.S. thesis, University of Arizona.

Johannsen, Albert, 1939, A descriptive petrography of the igneous rocks, Vol. I: University of Chicago Press.

Lance, J. F., 1959, Precambrian rocks of southeastern Arizona: Ariz. Geol. Soc. Guidebook II, p. 5.

Laughlin, A. W., 1960, Petrology of the Molino Basin area of the Santa Catalina Mountains, Arizona: M.S. thesis, University of Arizona.

Lindgren, W., 1933, Mineral Deposits: McGraw-Hill, New York.

McKee, E. D., 1951, Sedimentary basins of Arizona and adjoining areas: Geol. Soc. Am. Bull. vol. 62, p. 481.

Moore, B. N., et al, 1949, Geology of the Tucson Quadrangle, Arizona: U. S. Geological Survey open file report.

Pettijohn, F. J., 1957, Sedimentary Rocks: Harper Brothers, New York.

Peirce, F. L, 1958, Structure and petrography of part of the Santa Catalina Mountains: Ph.D. dissertation, University of Arizona.

Pilkington, H. D., 1961, A mineralogic investigation of some garnets from the Catalina Mountains, Pima County, Arizona: Ariz. Geol. Soc. Digest vol. IV, p. 117.

Raabe, R. G., 1959, Structure and petrography of the Bullock Canyon-Buehman Canyon area, Pima County, Arizona: M.S. thesis, University of Arizona.

Ramberg, Hans, 1952, The Origin of Metamorphic and Metasomatic Rocks: University of Chicago Press.

Sander, Bruno, 1930, Gefugekunde der Gesteine: Springer, Viena.

Shride, A. F., 1961, Some aspects of Younger Precambrian geology in southern Arizona: Ph.D. dissertation, University of Arizona.

Stoyanow, A. A., 1936, Correlation of Arizona Paleozoic formations: Geol. Soc. Am. Bull. vol. 47, p. 459.

Thompson, J. B., Jr., 1957, The graphical analysis of mineral assemblages in pelitic schists: Am. Miner. vol. 42, p. 842.

Turner, F. J., 1948, Mineralogical and structural evolution of the metamorphic rocks: Geol. Soc. Am. Memoir 30.

Turner, F. J., and Verhoogen, J., 1960, Igneous and Metamorphic Petrology, 2nd Ed: McGraw-Hill, New York.

Tuttle, O. F., and Bowen, N. L., 1958, Origin of granite in the light of experimental studies in the system $NaAlSi_3O_8$-$KAlSi_3O_8$-SiO_2-H_2O: Geol. Soc. Am. Memoir 74.

Wallace, R. M., 1954, Structures at the northern end of the Santa Catalina Mountains, Arizona: Ph.D. dissertation, University of Arizona.

Yoder, H. S., 1952, The MgO-Al_2O_3-SiO_2-H_2O system and the related metamorphic facies: Am. Jour. Sci., Bowen vol., p. 569.

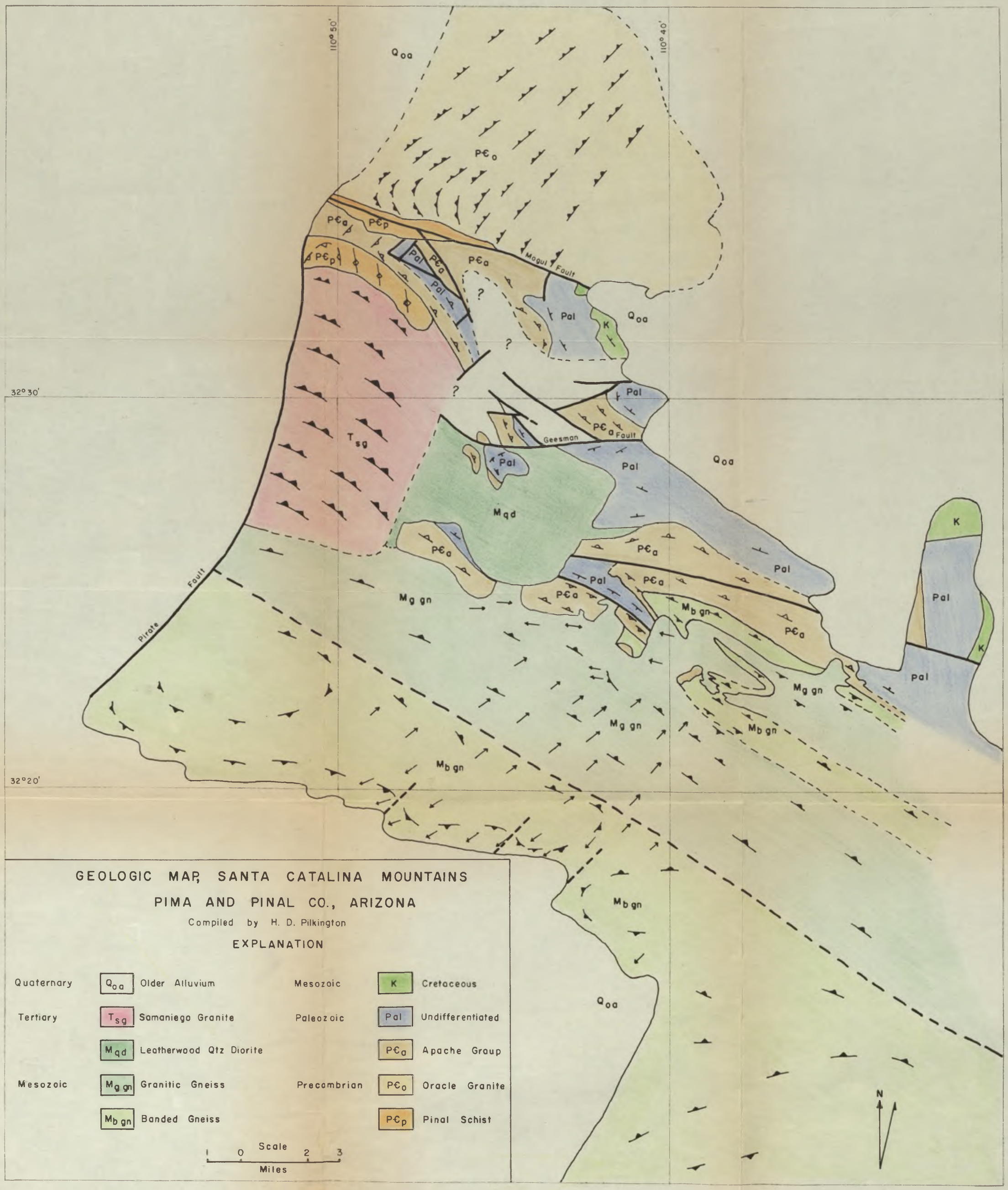

GEOLOGIC MAP, SANTA CATALINA MOUNTAINS
PIMA AND PINAL CO., ARIZONA

Compiled by H. D. Pilkington

EXPLANATION

Quaternary	Q_{oa}	Older Alluvium	Mesozoic	K	Cretaceous
Tertiary	T_{sg}	Samaniego Granite	Paleozoic	Pal	Undifferentiated
	M_{qd}	Leatherwood Qtz Diorite		$P\epsilon_a$	Apache Group
Mesozoic	$M_{g\,gn}$	Granitic Gneiss	Precambrian	$P\epsilon_o$	Oracle Granite
	$M_{b\,gn}$	Banded Gneiss		$P\epsilon_p$	Pinal Schist

Scale
1 0 2 3
Miles

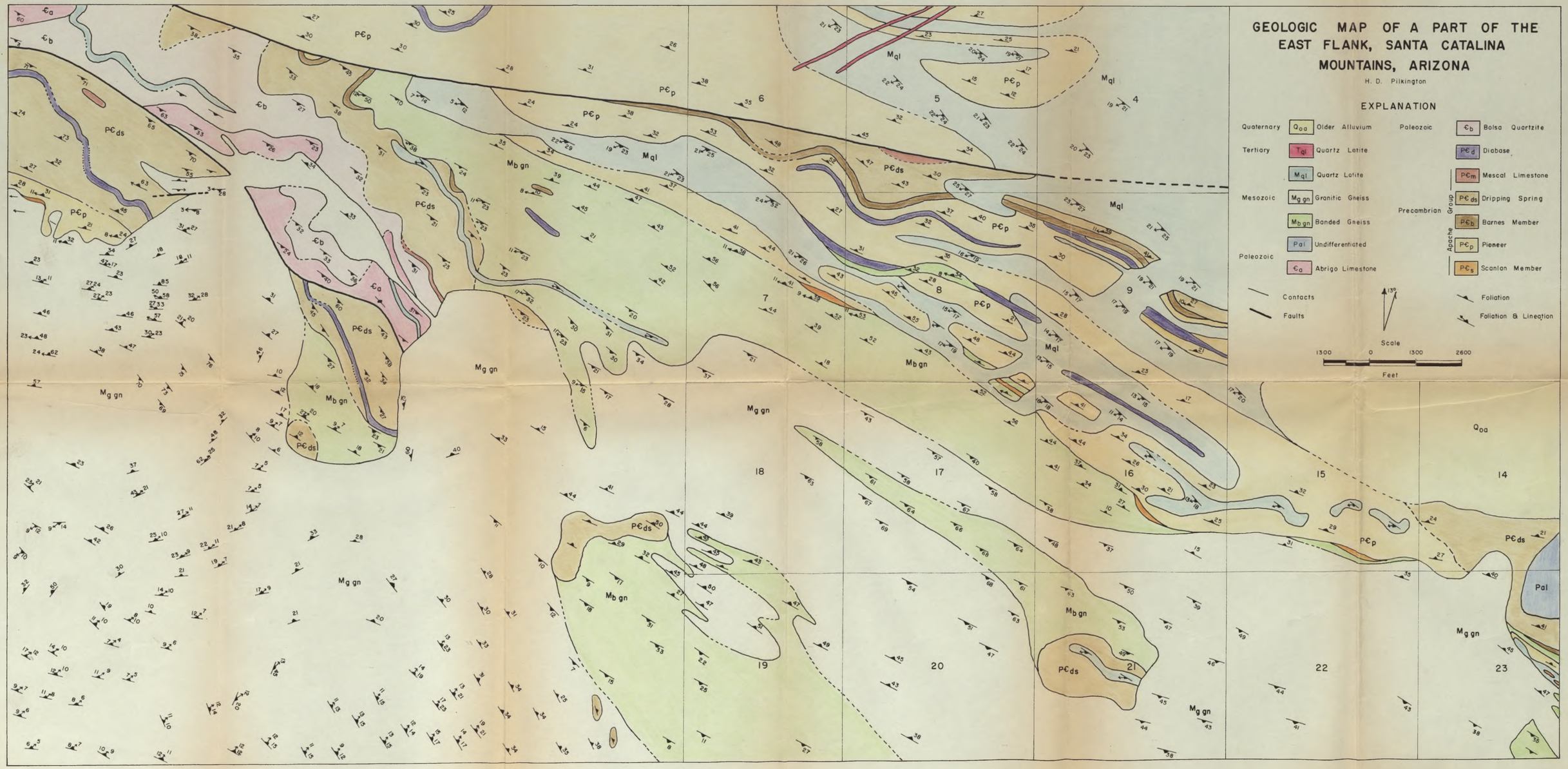

JOINT PATTERN OF A PART OF THE EAST FLANK, SANTA CATALINA MOUNTAINS, ARIZONA

H. D. Pilkington

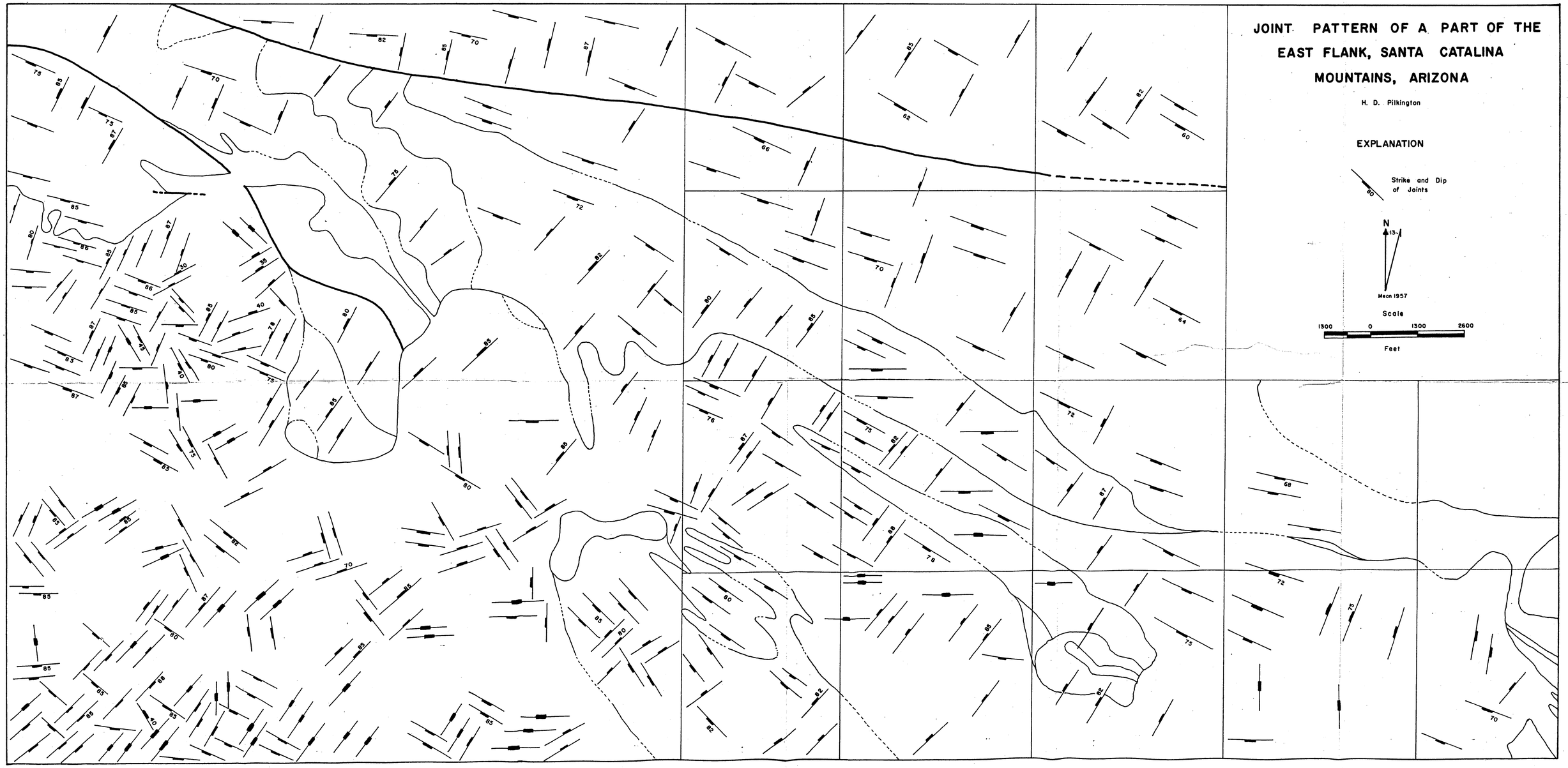

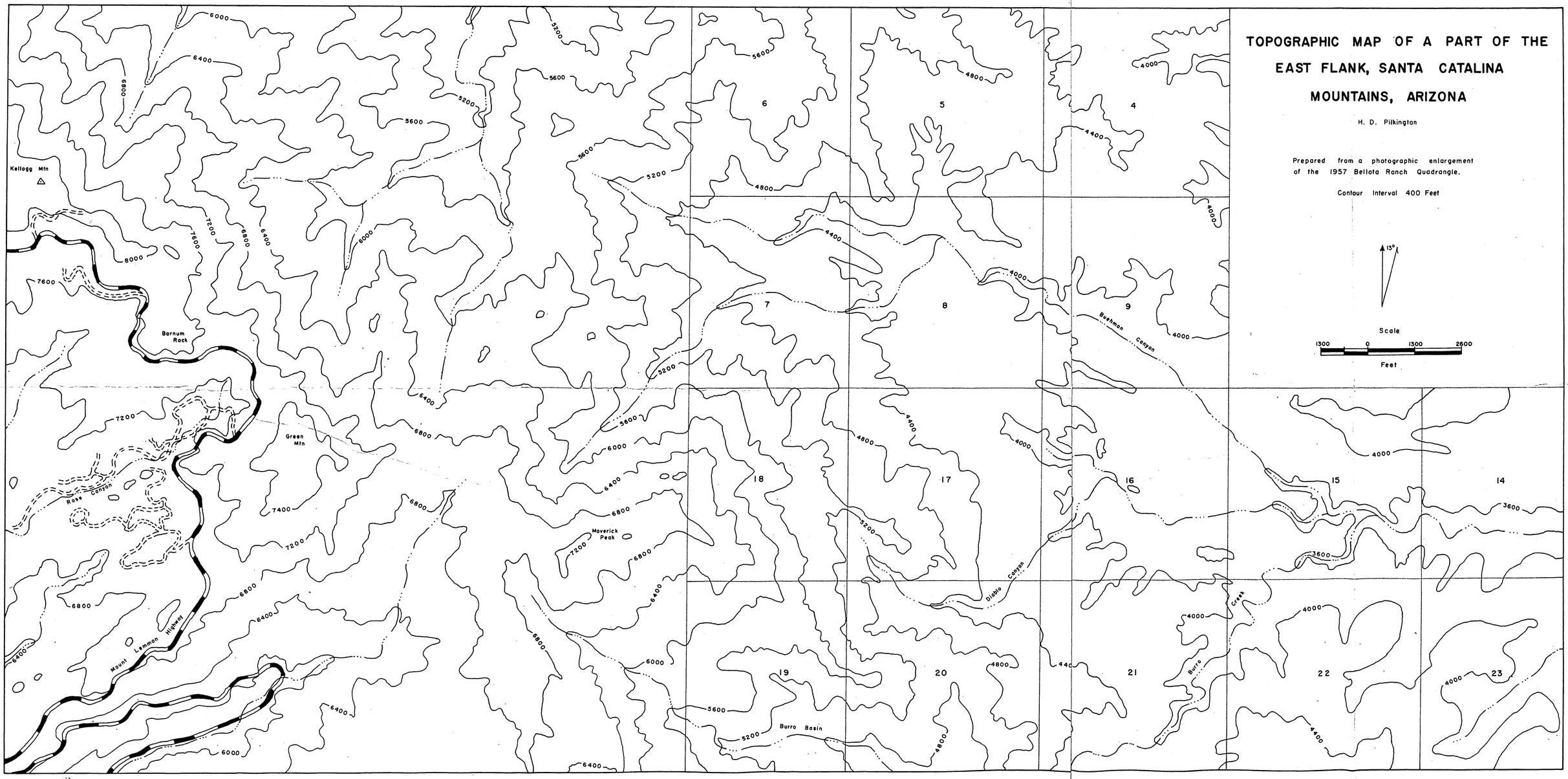

TOPOGRAPHIC MAP OF A PART OF THE EAST FLANK, SANTA CATALINA MOUNTAINS, ARIZONA

H. D. Pilkington

Prepared from a photographic enlargement of the 1957 Bellota Ranch Quadrangle.

Contour Interval 400 Feet

13°

Scale

1300 0 1300 2600

Feet